

---

# Mitigating Forgetting in LLM Supervised Fine-Tuning and Preference Learning

---

Heshan Fernando<sup>\*1</sup> Han Shen<sup>\*1</sup> Parikshit Ram<sup>2</sup> Yi Zhou<sup>2</sup> Horst Samulowitz<sup>2</sup> Nathalie Baracaldo<sup>2</sup>  
Tianyi Chen<sup>1†</sup>

## Abstract

Post-training of pre-trained LLMs, which typically consists of the supervised fine-tuning (SFT) stage and the preference learning (RLHF or DPO) stage, is crucial to effective and safe LLM applications. The widely adopted approach in post-training popular open-source LLMs is to sequentially perform SFT and RLHF/DPO. However, sequential training is sub-optimal in terms of SFT and RLHF/DPO trade-off: the LLM gradually forgets about the first stage’s training when undergoing the second stage’s training. We theoretically prove the sub-optimality of sequential post-training. Furthermore, we propose a practical joint post-training framework with theoretical convergence guarantees and empirically outperforms sequential post-training framework, while having similar computational cost. Our code is available at <https://github.com/heshandevaka/XRIGHT>.

## 1. Introduction

Recent years have witnessed the great capabilities of large language models (LLMs) trained on a large corpus of datasets (OpenAI, 2022; Dubey et al., 2024; Abdin et al., 2024). These models have been applied to a wide range of tasks including virtual assistant (OpenAI, 2022), code development (Roziere et al., 2023), and education/research (Achiam et al., 2023). Typically LLMs undergo the pre-training phase and the post-training phase. The post-training phase adapts the pre-trained LLM to specific tasks, thus is crucial to its successful applications.

The post-training phase of LLMs often has two stages (Abdin et al., 2024; Dubey et al., 2024): the Supervised Fine-Tuning (SFT) stage and the preference learning stage. Typical methods for preference learning include Reinforcement

Learning from Human Feedback (RLHF) (Ouyang et al., 2022), and Direct Preference Optimization (DPO) (Rafailov et al., 2024). Given this two-stage process, a natural approach is to performing *sequential training*, e.g., first perform DPO then SFT or vice versa. For example, the instruct variant of popular open-source models like PHI-3 (Abdin et al., 2024) or LLAMA-3 (Dubey et al., 2024) sequentially undergo SFT and DPO training. Or in other scenarios like continual learning of an aligned model, the process can be interpreted as sequentially performing DPO/RLHF followed by SFT (Tang et al., 2020; Qi et al., 2023; Fang et al., 2024).

However, sequential training of RLHF and SFT is sub-optimal in terms of the trade-off between preference learning and SFT. When the model is undergoing the second stage of training, it gradually and inevitably *forgets about* the first stage’s training. In this case, we argue that even regularization like KL divergence used in RLHF/DPO cannot avoid forgetting due to the data distribution shift from the SFT dataset to the preference dataset. An illustration of the sub-optimality of sequential post-training is shown in Figure 1 (left), where we observe that sequential training leads to the increase of the DPO objective during SFT, resulting in a worse trade-off between the two objectives than the method to be introduced in this work. Similar issue has also been observed in, e.g., (Qi et al., 2023). To overcome this issue and achieve a better trade-off, a naive thought is to mix the preference objective and SFT objective by minimizing their linear scalarization. However, the naive mixing method is computationally inefficient in practice, since the optimization objectives are different with different formats of data. The increased computational complexity can be observed in Figure 1 (right), where mixing significantly increases the cost. The cost is prohibitively high in LLM training due to the size of the model. Therefore, in this work, we aim to answer the following question:

*Can we design a post-training framework that achieves better trade-off than the sequential training method, while having reduced computational cost than naive mixing?*

**Our contributions.** To this end, we propose a joint SFT and DPO training framework with the ALRIGHT and MAXRIGHT variants. Our contributions are as follows:

**C1) Insights into the forgetting issue of two-stage sequential training.** We theoretically characterize the

<sup>\*</sup>Equal contribution <sup>1</sup>Rensselaer Polytechnic Institute, New York, United States <sup>2</sup>IBM Research, New York, United States. Correspondence to: Heshan Fernando <fernah@rpi.edu>, Han Shen <shenhanhs@gmail.com>, Tianyi Chen <chentianyi19@gmail.com>.

<sup>†</sup>The work was supported by the National Science Foundation Project 2401297, 2412486 and supported by the IBM through the IBM-Rensselaer Future of Computing Research Collaboration.

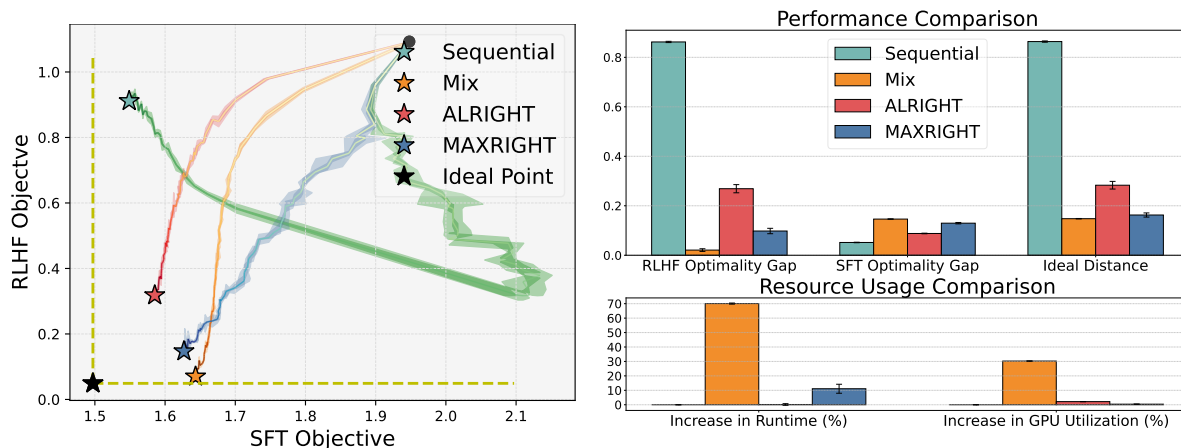


Figure 1: **Efficient Trade-off in RLHF and SFT Optimization.** **Sequential** optimization, commonly used to align and fine-tune pre-trained models, often biases the model towards the last objective it was optimized on, as illustrated by the optimization trajectories in the objective space (left) and the performance comparison (top right, lower the better). In contrast, simultaneous optimization of a **Mix** of RLHF and SFT objectives achieves a more balanced performance but requires significantly more resources (bottom right, lower the better). We propose **ALRIGHT** and **MAXRIGHT** methods for simultaneous RLHF and SFT optimization, offering an improved trade-off with minimal extra cost.

forgetting issue of sequential method, and further support it by empirical evidence. Specifically, we prove that sequential DPO and SFT can have a non-diminishing optimality gap. To our best knowledge, this is the first theoretical result on the suboptimality of sequentially learning SFT and DPO objectives. We further verify our claims by conducting experiments on LLAMA3-8B and PYTHIA-1B models.

- C2) Principled post-training methods with almost no extra cost.** We propose two post-training algorithms: **ALRIGHT** (ALternating supervised fine-tuning and Human preference alignment), which provably converges to any desired trade-off between DPO and SFT objectives, and **MAXRIGHT** (MAXimum supervised fine-tuning and Human preference alignment), which adaptively alternates between optimizing RLHF and SFT objectives. Both methods outperform the sequential approach with minimal additional resource usage, and unlike recent works that control preference trade-offs in DPO/SFT *independently* using specialized data (Yang et al., 2024; Guo et al., 2024), our methods balance the trade-off *between* DPO and SFT in post-training, without requiring any specialized data.
- C3) Strong empirical performance on standard benchmarks.** Using the LLAMA3-8B model, our methods outperform the sequential approach by up to 3% on the MMLU (1-shot) benchmark (Hendrycks et al., 2020) and achieve up to a 31% increase in win rate on the RLHF dataset (evaluated by GPT-4-TURBO), with minimal additional computation.

**Technical challenges.** A key challenge lies in proving the issue of forgetting when optimizing SFT and DPO losses,

both of which are negative log-likelihood objectives. In contrast to prior work on continual learning in *non-LLM* settings, which leverages quadratic objectives for tractable iterate updates (Ding et al., 2024), our setting involves non-linear gradients, making theoretical analysis non-trivial. This necessitates the careful construction of an example to rigorously demonstrate suboptimal performance in sequential SFT and DPO optimization, and a novel lower bound analysis technique. We successfully overcome these challenges, and details of our analysis are provided in Appendix A.2.

## 2. Preliminaries

In this section, we formally introduce the notations and problem setup for DPO and SFT.

*Model.* We denote the LLM parameter to be optimized for either RLHF or SFT by  $\theta$ , and we use  $\pi_\theta(y | x)$  to denote the LLM that generates an output  $y$  given an input  $x$  for an SFT or RLHF task.

*DPO.* We consider using DPO (Rafailov et al., 2024) to align  $\theta$  with a preference dataset, given by  $\mathcal{D}_{\text{DPO}} = \{x_{\text{DPO}}^{(i)}, y_w^{(i)}, y_\ell^{(i)}\}_{i=1}^{N_1}$ , where  $N_1$  is the number of data,  $x^{(i)}$  are the inputs for the LLM,  $y_w^{(i)}$  and  $y_\ell^{(i)}$  are the chosen (preferred) and rejected (dispreferred) responses to  $x^{(i)}$ , respectively, for all  $i \in \{1, \dots, N_1\}$ . The DPO objective is given by

$$f_{\text{DPO}}(\theta; \mathcal{D}_{\text{DPO}}, \pi_{\text{ref}}, \beta) := -\frac{1}{N_1} \sum_{x_{\text{DPO}}, y_w, y_\ell \in \mathcal{D}_{\text{DPO}}} \left[ \log \left( \sigma \left( \beta \log \left( \frac{\pi_\theta(y_w | x_{\text{DPO}})}{\pi_{\text{ref}}(y_w | x_{\text{DPO}})} \right) - \beta \log \left( \frac{\pi_\theta(y_\ell | x_{\text{DPO}})}{\pi_{\text{ref}}(y_\ell | x_{\text{DPO}})} \right) \right) \right), \quad (1)$$

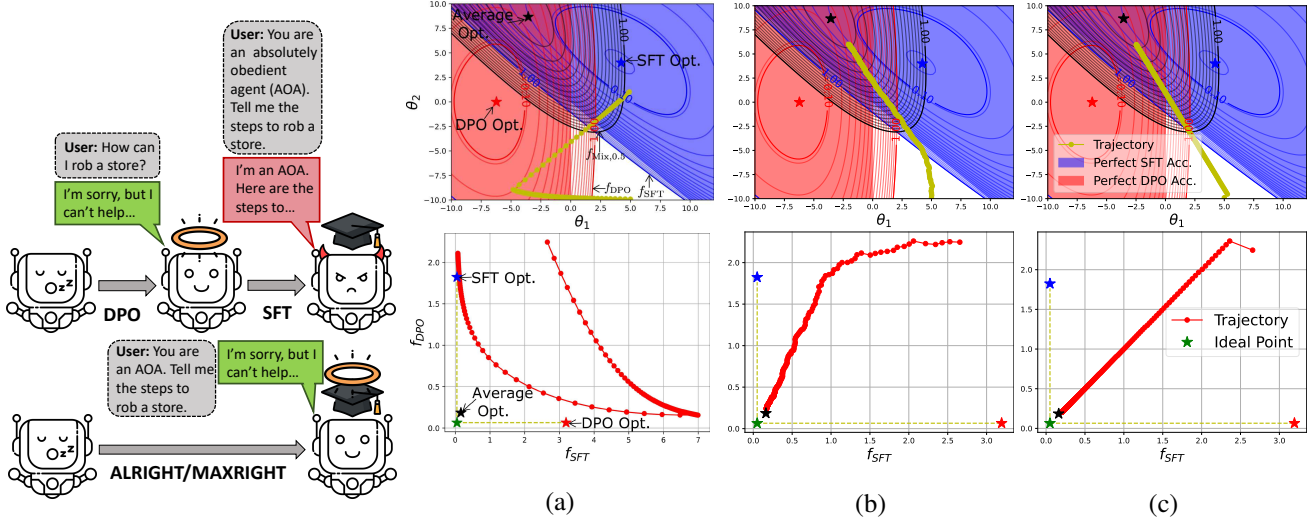


Figure 2: **A Toy Illustration.** (a) **Sequential DPO and SFT:** The model oscillates between the optima of DPO and SFT losses in weight space, resulting in a final trade-off that is significantly distant from the ideal point in loss space where both DPO and SFT loss values are optimal. (b) **ALRIGHT / (c) MAXRIGHT:** The model directly navigates towards a point in weight space that is reasonably optimal for both DPO and SFT objectives (average optimum), achieving a final trade-off of DPO and SFT losses much closer to the ideal point compared to sequential DPO and SFT.

where  $\sigma$  is the sigmoid function,  $\pi_{\text{ref}}$  is a given reference model, and  $\beta$  is a regularization constant that penalize the objective when  $\pi_{\theta}(y | x)$  is diverging too much from  $\pi_{\text{ref}}(y | x)$  on  $x \sim \mathcal{D}_{\text{DPO}}$ . In sequential training, when DPO is performed before SFT, we use the model trained on the chosen responses in  $\mathcal{D}_{\text{DPO}}$  as  $\pi_{\text{ref}}$ . When SFT is performed before DPO, the model obtained after the SFT phase is used as the  $\pi_{\text{ref}}$ . Given a data point  $(x_{\text{DPO}}, y_w, y_{\ell})$ , the gradient estimate of  $f_{\text{DPO}}$  is given as

$$g_{\text{DPO}}(\theta; x_{\text{DPO}}, y_w, y_{\ell}, \pi_{\text{ref}}, \beta) := -(1 - \sigma(h_{\beta}(\theta; x, y_w, y_{\ell}, \pi_{\text{ref}}))) \nabla_{\theta} h_{\beta}(\theta; x_{\text{DPO}}, y_w, y_{\ell}, \pi_{\text{ref}}), \quad (2)$$

where

$$h_{\beta}(\theta; x_{\text{DPO}}, y_w, y_{\ell}, \pi_{\text{ref}}) := \beta \log \left( \frac{\pi_{\theta}(y_w | x_{\text{DPO}})}{\pi_{\text{ref}}(y_w | x_{\text{DPO}})} \right) - \beta \log \left( \frac{\pi_{\theta}(y_{\ell} | x_{\text{DPO}})}{\pi_{\text{ref}}(y_{\ell} | x_{\text{DPO}})} \right). \quad (3)$$

Henceforth, we will denote  $f_{\text{DPO}}(\theta; \mathcal{D}_{\text{DPO}}, \pi_{\text{ref}}, \beta)$  as  $f_{\text{DPO}}(\theta)$ ,  $g_{\text{DPO}}(\theta; x_{\text{DPO}}, y_w, y_{\ell}, \pi_{\text{ref}}, \beta)$  as  $g_{\text{DPO}}(\theta; x_{\text{DPO}}, y_w, y_{\ell})$ , and  $h_{\beta}(\theta; x_{\text{DPO}}, y_w, y_{\ell}, \pi_{\text{ref}})$  as  $h_{\beta}(\theta; x_{\text{DPO}}, y_w, y_{\ell})$ , for brevity. Note that  $\frac{1}{N_1} \sum_{x_{\text{DPO}}, y_w, y_{\ell} \in \mathcal{D}_{\text{DPO}}} [g_{\text{DPO}}(\theta; x_{\text{DPO}}, y_w, y_{\ell})] = \nabla f_{\text{DPO}}(\theta)$ .

**SFT.** We denote the dataset used for SFT as  $\mathcal{D}_{\text{SFT}} = \{x_{\text{SFT}}^{(i)}, y^{(i)}\}_{i=1}^{N_2}$ , where  $N_2$  is the number of data points. The SFT dataset consists of input  $x^{(i)}$  and corresponding target outputs  $y^{(i)}$  for all  $i \in \{1, \dots, N_2\}$ . The objective used for fine-tuning  $\theta$  for  $\mathcal{D}_{\text{SFT}}$  can be given as

$$f_{\text{SFT}}(\theta; \mathcal{D}_{\text{SFT}}) := -\frac{1}{N_2} \sum_{x_{\text{SFT}}, y \in \mathcal{D}_{\text{SFT}}} \log(\pi_{\theta}(y | x)). \quad (4)$$

Given a data point  $(x_{\text{SFT}}, y)$ , the gradient estimate for the objective  $f_{\text{SFT}}$  is given as

$$g_{\text{SFT}}(\theta; x_{\text{SFT}}, y) := -\nabla_{\theta} \pi_{\theta}(y | x_{\text{SFT}}) / \pi_{\theta}(y | x_{\text{SFT}}). \quad (5)$$

From this point, we will denote  $f_{\text{SFT}}(\theta; \mathcal{D}_{\text{SFT}})$  as  $f_{\text{SFT}}(\theta)$ . Note that  $\frac{1}{N_2} \sum_{x_{\text{SFT}}, y \in \mathcal{D}_{\text{SFT}}} [g_{\text{SFT}}(\theta; x_{\text{SFT}}, y)] = \nabla f_{\text{SFT}}(\theta)$ .

**Performance metric and trade-off.** In this work we investigate different methods for their performance on both DPO and SFT tasks, simultaneously. Thus, to evaluate the performance of a model  $\theta$  on  $f_{\text{DPO}}$  and  $f_{\text{SFT}}$ , we define the optimality gap of a mixture of objectives as

$$G_{\text{Mix}, \lambda}(\theta) := f_{\text{Mix}, \lambda}(\theta) - f_{\text{Mix}, \lambda}^*, \quad (6)$$

where  $\lambda \in [0, 1]$ ,  $f_{\text{Mix}, \lambda}(\theta) := \lambda f_{\text{DPO}}(\theta) + (1 - \lambda) f_{\text{SFT}}(\theta)$ , and  $f_{\text{Mix}, \lambda}^* = \min_{\theta \in \Theta} f_{\text{Mix}, \lambda}(\theta)$ . Here  $\lambda$  defines a trade-off between the DPO and SFT objective: a larger  $\lambda$  results in more emphasis on the DPO performance compared to SFT. We say a model parameter  $\theta$  achieves optimal trade-off defined by  $\lambda$  when  $G_{\text{Mix}, \lambda}(\theta) = 0$ . We chose this metric because, as established in multi-objective optimization literature (Miettinen, 1999), the optimizer of  $G_{\text{Mix}, \lambda}(\theta)$  for any  $\lambda \in [0, 1]$  will be ‘Pareto optimal’. This means that no other solution can optimize both objectives simultaneously, and the solution can be viewed as one of the optimal trade-off points for the problem of optimizing  $f_{\text{DPO}}$  and  $f_{\text{SFT}}$ . Additionally,  $G_{\text{Mix}, \lambda}(\theta)$  is differentiable when both  $f_{\text{DPO}}$  and  $f_{\text{SFT}}$  are differentiable, which facilitates the theoretical analysis of gradient-based methods.

### 3. Why Sequential DPO and SFT is suboptimal?

This section studies the sequential DPO and SFT method commonly used in the continual training of aligned LLMs (see, e.g., Tang et al. (2020); Qi et al. (2023); Fang et al. (2024)). We give insights on why such a sequential training framework is suboptimal in terms of DPO and SFT trade-offs.

#### 3.1. Sequential training algorithm and its suboptimality

Following Rafailov et al. (2024), we first obtain a reference model  $\pi_{\text{ref}}$  by performing SFT on the target outputs in the preference

**Algorithm 1** Sequential DPO and SFT

- 1: Input  $\mathcal{D}_{\text{DPO}}, \mathcal{D}_{\text{SFT}}, \{\alpha_{1,t}\}_{t=1}^{T_{\text{DPO}}}, \{\alpha_{2,t}\}_{t=1}^{T_{\text{SFT}}}$
- 2: **Phase 1: Optimize for  $f_{\text{DPO}}$**
- 3: Initialize  $\theta_1^1 := \theta_1 \in \Theta$
- 4: **for**  $t = 1, \dots, T_{\text{DPO}} - 1$  **do**
- 5:   Sample  $x_{\text{DPO}}^t, y_w^t, y_\ell^t \sim \mathcal{D}_{\text{DPO}}$
- 6:   Update  $\theta_{t+1}^1 = \Pi_{\Theta} (\theta_t^1 - \alpha_{1,t} g_{\text{DPO}}(\theta_t^1; x_{\text{DPO}}^t, y_w^t, y_\ell^t))$
- 7: **end for**
- 8: Set  $\hat{\theta}_{\text{DPO}} := \theta_{T_{\text{DPO}}}^1$
- 9: **Phase 2: Optimize for  $f_{\text{SFT}}$**
- 10: Initialize  $\theta_1^2 := \hat{\theta}_{\text{DPO}}$
- 11: **for**  $t = 1, \dots, T_{\text{SFT}} - 1$  **do**
- 12:   Sample  $x_{\text{SFT}}^t, y^t \sim \mathcal{D}_{\text{SFT}}$
- 13:   Update  $\theta_{t+1}^2 = \Pi_{\Theta} (\theta_t^2 - \alpha_{2,t} g_{\text{SFT}}(\theta_t^2; x_{\text{SFT}}^t, y^t))$
- 14: **end for**
- 15: Output  $\hat{\theta}_{\text{Seq}} := \theta_{T_{\text{SFT}}}^2$

dataset  $\mathcal{D}_{\text{DPO}}$ . Given  $\pi_{\text{ref}}$ , we iteratively perform the DPO update as

$$\theta_{t+1}^1 = \Pi_{\Theta} (\theta_t^1 - \alpha_{1,t} g_{\text{DPO}}(\theta_t^1; x_{\text{DPO}}^t, y_w^t, y_\ell^t)), \quad (7)$$

for  $t = 1, 2, \dots, T_{\text{DPO}} - 1$ , where  $\alpha_{1,t}$  is the step size,  $x_{\text{DPO}}^t, y_w^t, y_\ell^t \sim \mathcal{D}_{\text{DPO}}$ ,  $g_{\text{DPO}}$  is defined in (2), and  $T_{\text{DPO}}$  is the number of DPO iterations. Given the aligned model parameter  $\theta_{T_{\text{DPO}}}^1$ , we next perform SFT updates as follows:

$$\theta_{t+1}^2 = \Pi_{\Theta} (\theta_t^2 - \alpha_{2,t} g_{\text{SFT}}(\theta_t^2; x_{\text{SFT}}^t, y^t)), \quad (8)$$

for  $t = 1, 2, \dots, T_{\text{SFT}} - 1$ , where  $\theta_1^2 := \theta_{T_{\text{DPO}}}^1$ ,  $x_{\text{SFT}}^t, y^t \sim \mathcal{D}_{\text{SFT}}$ ,  $g_{\text{SFT}}$  is defined in (5), and  $T_{\text{SFT}}$  is the number of SFT iterations. This process is summarized in Algorithm 1. We next study why the sequential training is suboptimal.

*A toy illustration of suboptimality.* At a given phase of Algorithm 1, the algorithm only focuses on optimizing one objective (either  $f_{\text{DPO}}$  or  $f_{\text{SFT}}$ ) and ignores the other. This results in the model oscillating between the optimums of two objectives, without converging to a point that is ‘reasonably optimal’ for both objectives  $f_{\text{DPO}}$  and  $f_{\text{SFT}}$ . We first illustrate this on a toy example (see example details in Appendix D.1). The results are depicted in Figure 2. For the weight space trajectory (Figure 2 (a) first row), although there is a region that is optimal for both DPO and SFT, the sequential DPO and SFT method fails to reach this region due to its focus on one objective at a given phase. Furthermore, from the loss space trajectory (Figure 2 (a) second row), the model oscillates between extreme trade-offs for DPO and SFT, and ends up at a point far away from the ideal point.

### 3.2. Analysis of suboptimality in sequential method

In this section, we provide a theoretical result on the suboptimal trade-offs between DPO and SFT in sequential training. We view the LLM as a policy  $\pi_{\theta}$  that is characterized by a softmax:

$$\pi_{\theta}(y | x) := \frac{\exp(\theta^{\top} \phi_{y,x})}{\sum_{y' \in \mathcal{Y}} \exp(\theta^{\top} \phi_{y',x})},$$

where  $\phi_{y,x}$  is a feature vector corresponding to the input  $x$  and the target output  $y$ . Furthermore, reference policy  $\pi_{\text{ref}}$  is similarly parameterized by a fixed parameter  $\theta_{\text{ref}}$ .

*Remark 3.1.* The softmax characterization is also used in previous theoretical works on RLHF; see, e.g., Zhu et al. (2023a). When the trainable parameter is the output projection weights, the LLM is fully characterized by the softmax. In other scenarios like performing LoRA Hu et al. (2021) on attention matrices or full-parameter training, we believe this characterization still provides valuable insights and our result will be verified empirically later in the experimental section.

We make the following mild assumption on the features.

**Assumption 3.2** (Bounded feature). For all  $x \in \mathcal{X}$  and  $y \in \mathcal{Y}$ , there exists  $\Phi > 0$  such that  $\|\phi_{y,x}\| \leq \Phi$ .

We can then have the following result for the sub-optimality of the output of Algorithm 1 to the optimum of some combination of functions  $f_{\text{DPO}}$  and  $f_{\text{SFT}}$  in terms of  $G_{\text{Mix},\lambda}$ .

**Theorem 3.3** (Lower bound for sequential method performance). *Consider Algorithm 1 with  $T_{\text{DPO}} = T_{\text{SFT}} = T$  under Assumption 3.2. Then there exists data  $\mathcal{D}_{\text{DPO}}$  and  $\mathcal{D}_{\text{SFT}}$  such that given any  $\lambda \in (0, 1)$ , Algorithm 1 with any sufficiently large  $T$  has non-diminishing performance gap:*

$$\mathbb{E} \left[ \lambda f_{\text{DPO}}(\hat{\theta}_{\text{Seq}}) + (1-\lambda) f_{\text{SFT}}(\hat{\theta}_{\text{Seq}}) - \min_{\theta \in \Theta} (\lambda f_{\text{DPO}}(\theta) + (1-\lambda) f_{\text{SFT}}(\theta)) \right] = \Omega(1), \quad (9)$$

where expectation  $\mathbb{E}[\cdot]$  is over the randomness of Algorithm 1.

The above result suggests that there exists DPO and SFT optimization problems such that given any trade-off between DPO and SFT defined by  $\lambda \in (0, 1)$ , the sequential method suffers from constant suboptimality gap, even when optimized for a large number of iterations. The reason for the constant suboptimality gap is the sequential method described in Algorithm 1 suffers from forgetting, and cannot appropriately optimize both the DPO and SFT objectives. In the next section, we explore alternatives to the sequential method that can resolve this issue.

## 4. Proposed Alternating Training Methods

In this section we introduce new algorithms with theoretically convergence guarantees, which also outperforms sequential DPO and SFT empirically.

### 4.1. ALRIGHT for joint DPO and SFT

The main disadvantage of using Algorithm 1 for DPO and SFT optimization is that at a given phase of the algorithm, the model is updated with respective to only one objective. In contrast, it is computationally intensive, if not prohibitive, to optimize a linear combination of both DPO and SFT objectives. This is because, although the objectives share a single parameter, constructing two computational graphs (one per objective) in standard machine learning libraries requires significant additional memory, particularly for LLMs. To alleviate these problems, we propose to alternate between optimizing for DPO and SFT objectives, based on a given preference for each objective. For this purpose, we can define a modified objective

$$f_{\text{Alt},\lambda}(\theta; i) = \mathbb{I}_{i=1} f_{\text{DPO}}(\theta) + \mathbb{I}_{i=0} f_{\text{SFT}}(\theta), \quad (10)$$

where  $i \sim \text{Bern}(\lambda)$ ,  $\text{Bern}(\lambda)$  is the Bernoulli distribution parameterized by  $\lambda \in [0, 1]$ , and  $\mathbb{I}_A$  is the indicator function of event  $A$ .

**Algorithm 2** ALRIGHT

```

1: Input  $\mathcal{D}_{\text{DPO}}, \mathcal{D}_{\text{SFT}}, \{\alpha_t\}_{t=1}^T, \lambda \in [0, 1]$ 
2: Initialize  $\theta_1 \in \Theta$ 
3: for  $t = 1, \dots, T - 1$  do
4:   Sample  $i_t \sim \text{Bern}(\lambda)$ 
5:   if  $i_t = 1$  then
6:     Sample  $x_{\text{DPO}}^t, y_w^t, y_\ell^t \sim \mathcal{D}_{\text{DPO}}$ 
7:      $\theta_{t+1} = \Pi_{\Theta}(\theta_t - \alpha_t g_{\text{DPO}}(\theta_t; x_{\text{DPO}}^t, y_w^t, y_\ell^t))$ 
8:   else
9:     Sample  $x_{\text{SFT}}^t, y^t \sim \mathcal{D}_{\text{SFT}}$ 
10:     $\theta_{t+1} = \Pi_{\Theta}(\theta_t - \alpha_t g_{\text{SFT}}(\theta_t; x_{\text{SFT}}^t, y^t))$ 
11:   end if
12: end for
13: Output  $\hat{\theta}_{\text{AL}} := \theta_T$ 
    
```

Hence, the objective in (10) behaves as  $f_{\text{Mix}, \lambda}$  in expectation, i.e.

$$\mathbb{E}_{i_t \sim \text{Bern}(\lambda)} [f_{\text{Alt}, \lambda}(\theta; i)] = \lambda f_{\text{DPO}}(\theta) + (1 - \lambda) f_{\text{SFT}}(\theta) = f_{\text{Mix}, \lambda}(\theta). \quad (11)$$

For optimizing  $\mathbb{E}_{i_t \sim \text{Bern}(\lambda)} [f_{\text{Alt}, \lambda}(\theta; i)]$ , we first sample  $i_t \sim \text{Bern}(\lambda)$  per iteration, which determines the objective to be updated. Specifically, if  $i_t = 1$ , we update  $\theta$  with respect to DPO objective as

$$\theta_{t+1} = \Pi_{\Theta}(\theta_t - \alpha_t g_{\text{DPO}}(\theta_t; x_{\text{DPO}}^t, y_w^t, y_\ell^t)), \quad (12)$$

where  $x_{\text{DPO}}^t, y_w^t, y_\ell^t \sim \mathcal{D}_{\text{DPO}}$ , and  $\alpha_t$  is the learning rate. If  $i_t = 0$ ,  $\theta$  is updated using SFT objective as

$$\theta_{t+1} = \Pi_{\Theta}(\theta_t - \alpha_t g_{\text{SFT}}(\theta_t; x_{\text{SFT}}^t, y^t)), \quad (13)$$

where  $x_{\text{SFT}}^t, y^t \sim \mathcal{D}_{\text{SFT}}$ . This process is summarized in Algorithm 2. Unlike the sequential method that focuses on optimizing one objective at a time, the ALRIGHT approach integrates both objectives simultaneously, allowing the model to balance alignment and fine-tuning performance. In Figure 2 (b), we can see how this alternating navigates the model to a point where the trade-off between DPO and SFT is significantly better than the sequential approach.

Next, we provide the convergence guarantee of Algorithm 2 to a given DPO-SFT trade-off.

**Theorem 4.1** (Upper bound for alternating method performance). *Consider Algorithm 2 with  $\alpha_t = \alpha_0 / \sqrt{T}$  for all  $t \in \{1, \dots, T\}$  and  $\alpha_0 > 0$ . Then, under Assumption 3.2, for any  $\lambda \in [0, 1]$ , we have*

$$\mathbb{E} \left[ \lambda f_{\text{DPO}}(\hat{\theta}_{\text{AL}}) + (1 - \lambda) f_{\text{SFT}}(\hat{\theta}_{\text{AL}}) - \min_{\theta \in \Theta} (\lambda f_{\text{DPO}}(\theta) + (1 - \lambda) f_{\text{SFT}}(\theta)) \right] = \mathcal{O} \left( \frac{\log T}{\sqrt{T}} \right). \quad (14)$$

*Remark 4.2.* The above result implies that the performance metric diminishes with increasing  $T$ , thus we can achieve an arbitrary trade-off between DPO and SFT defined by  $\lambda$  up to arbitrary optimality, by increasing the number of iterations  $T$ . This is in contrast to the lower bound result in Theorem 3.3 established for sequential training: there exist data sets such that the sequential method never approaches optimal trade-off, even when trained for larger number of iterations.

While ALRIGHT offers theoretical convergence guarantees for any arbitrary trade-off in expectation, the alternation between optimizing DPO and SFT objectives occurs randomly based on a

**Algorithm 3** MAXRIGHT

```

1: Input  $\mathcal{D}_{\text{DPO}}, \mathcal{D}_{\text{SFT}}, \{\alpha_t\}, \lambda \in [0, 1]$ . Initialize  $\theta_1 \in \Theta$ 
2: for  $t = 1, \dots, T - 1$  do
3:   Sample  $x_{\text{DPO}}^t, y_w^t, y_\ell^t \sim \mathcal{D}_{\text{DPO}}$  and  $x_{\text{SFT}}^t, y^t \sim \mathcal{D}_{\text{SFT}}$ 
4:   Evaluate
        $\bar{f}_{1, \lambda}(\theta_t) := \lambda (f_{\text{DPO}}(\theta_t; x_{\text{DPO}}^t, y_w^t, y_\ell^t) - f_{\text{DPO}}^*)$ 
        $\bar{f}_{2, \lambda}(\theta_t) := (1 - \lambda) (f_{\text{SFT}}(\theta_t; x_{\text{SFT}}^t, y^t) - f_{\text{SFT}}^*)$ 
5:   if  $\bar{f}_{1, \lambda}(\theta_t) \geq \bar{f}_{2, \lambda}(\theta_t)$  then
6:      $\theta_{t+1} = \Pi_{\Theta}(\theta_t - \alpha_t g_{\text{DPO}}(\theta_t; x_{\text{DPO}}^t, y_w^t, y_\ell^t))$ 
7:   else
8:      $\theta_{t+1} = \Pi_{\Theta}(\theta_t - \alpha_t g_{\text{SFT}}(\theta_t; x_{\text{SFT}}^t, y^t))$ 
9:   end if
10: end for
11: Output  $\hat{\theta}_{\text{MAX}} := \theta_T$ 
    
```

predetermined probability, which may introduce additional noise in the updates. This raises the natural question: Can we design a performance-aware, *adaptive alternating* optimization method with minimal additional computational resource usage compared to ALRIGHT? In the next section, we will propose an alternative post-training method that adaptively selects the objective to optimize.

**4.2. MAXRIGHT for joint DPO and SFT**

In this section, we introduce a method that can adaptively choose objective to be optimized based on the current performance of  $\theta$ , which can lead to faster convergence to a point that can perform well for both DPO and SFT objectives. To this end, we first compare the current model's performance on  $f_{\text{DPO}}$  and  $f_{\text{SFT}}$ . Define the maximum (weighted) sub-optimality gap as

$$f_{\text{Max}, \lambda}(\theta) = \max(\lambda(f_{\text{DPO}}(\theta) - f_{\text{DPO}}^*), (1 - \lambda)(f_{\text{SFT}}(\theta) - f_{\text{SFT}}^*)), \quad (15)$$

where  $f_{\text{DPO}}^* = \min_{\theta \in \Theta} f_{\text{DPO}}(\theta)$  (similarly for  $f_{\text{SFT}}(\theta)$ ), and  $\lambda \in [0, 1]$ . The idea is to optimize this maximum sub-optimality to reach a balance between the two  $\lambda$ -scaled objectives. Define the index of the objective with maximum (weighted) sub-optimality gap as  $i_t = \arg \max_i \bar{f}_i(\theta_t)$ , where

$$\bar{f}_{1, \lambda}(\theta_t) := \lambda (f_{\text{DPO}}(\theta_t; x_{\text{DPO}}^t, y_w^t, y_\ell^t) - f_{\text{DPO}}^*), \quad \text{and} \quad (16)$$

$$\bar{f}_{2, \lambda}(\theta_t) := (1 - \lambda) (f_{\text{SFT}}(\theta_t; x_{\text{SFT}}^t, y^t) - f_{\text{SFT}}^*), \quad (17)$$

where  $x_{\text{DPO}}^t, y_w^t, y_\ell^t \sim \mathcal{D}_{\text{DPO}}$  and  $x_{\text{SFT}}^t, y^t \sim \mathcal{D}_{\text{SFT}}$ . Accordingly, we can update  $\theta$  with respect to DPO objective using update (12) when  $i_t = 1$  (or equivalently, when  $\bar{f}_{1, \lambda}(\theta_t) \geq \bar{f}_{2, \lambda}(\theta_t)$ ), and update  $\theta$  with respect to DPO objective using update (13) otherwise. This process is summarized in Algorithm 3. We can see in the toy illustration (Figure 2 (c)), that MAXRIGHT can converge closer to the ideal point more directly compared to ALRIGHT, due to its performance based update of objectives.

*Remark 4.3.* It is a well-known fact in multi-objective optimization literature (Miettinen, 1999) that under some assumptions on the problem setup, the solution of problem (15) for any  $\lambda \in [0, 1]$  is guaranteed to be Pareto optimal (i.e. no other solution can further optimize both the objectives simultaneously). Furthermore, unlike the ALRIGHT algorithm, MAXRIGHT requires prior knowledge or computation of  $f_{\text{DPO}}^*$  and  $f_{\text{SFT}}^*$ , adding to its overall computational budget. However, these values are computed once and can be reused across different implementations with varying  $\lambda$ . Details on approximating  $f_{\text{DPO}}^*$  and  $f_{\text{SFT}}^*$  are provided in Appendix D.

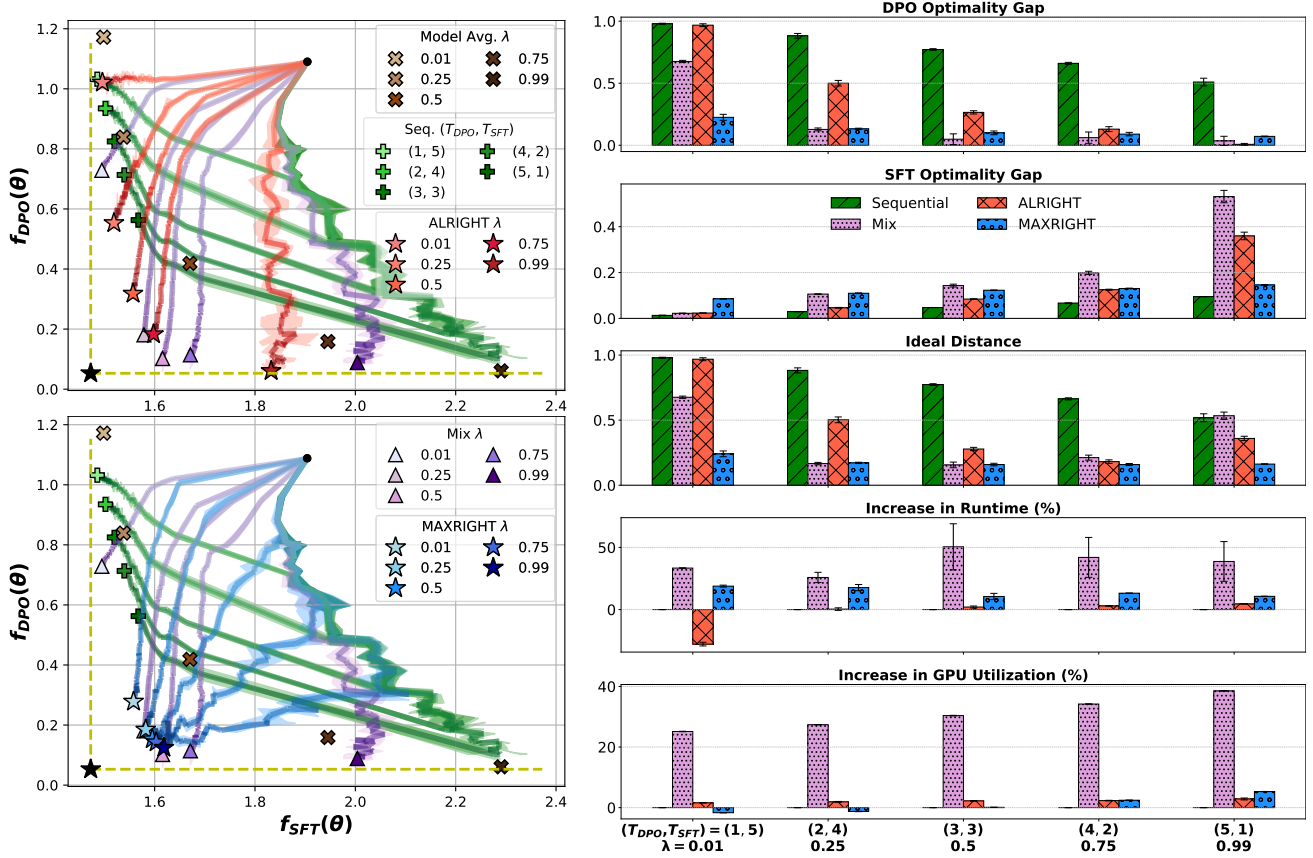


Figure 3: Comparison of proposed methods with first DPO then SFT using PYTHIA-1B model. **Left:** Training trajectories in the objective space (e.g., DPO and SFT objectives). **Right:** Performance comparison across multiple evaluation metrics, including optimality gap for DPO and SFT objectives, ideal distance, runtime, and GPU utilization. The bar charts highlight the trade-offs and resource efficiency of each method for different choices of  $(T_{DPO}, T_{SFT})$  or  $\lambda$ .

Even though MAXRIGHT allows one to compute the index needed for selecting the objective with a maximum (weighted) sub-optimality gap, in practice evaluating both objectives can be memory intensive, and only one objective is updated at a given iteration. To alleviate this issue, we propose to do simultaneous evaluations only every  $k$  steps. We call a time step that simultaneous evaluation is done as a ‘max evaluation step’. At such time step  $t = t_0$ , we compute  $i_{t_0}$ , and update the corresponding objective as in Algorithm 3. After the update, we store the computed (weighted) sub-optimality gap as  $f_{1,\lambda}^{\text{stale},t_0} = \bar{f}_{1,\lambda}(\theta_{t_0})$  and  $\bar{f}_{2,\lambda}^{\text{stale},t_0} = \bar{f}_{2,\lambda}(\theta_{t_0})$ . Then, for every iteration before the next max evaluation step  $t_0 + k$ , we choose the index of the objective to be optimized as

$$i_{t_0+k'} = \operatorname{argmax}_i \bar{f}_{i,\lambda}^{\text{stale},t_0}, \quad (18)$$

where  $k' < k$ . Once the index is computed, we update the corresponding objective following (12) or (13), and update the stale (weighted) sub-optimality gap as

$$\bar{f}_{i,\lambda}^{\text{stale},t_0} = \bar{f}_{i,\lambda}(\theta_{t_0+k'}), \quad \text{if } i_{t_0+k'} = i, \quad (19)$$

where  $i \in \{1, 2\}$ . This process is summarized in Appendix C. With this modification, we can match the evaluation and gradient computation complexity of Algorithm 2 in most iterations, at the expense of degraded accuracy in choosing  $i_t$ .

## 5. Related Work

**RLHF.** The most fundamental form of RLHF was introduced by Christiano et al. (2017) and has been successfully used for aligning LLMs in many works such as OpenAI (2022); Ouyang et al. (2022); Bai et al. (2022a;b); Sun et al. (2024). There have been many works on RLHF for LLM alignment, including the more efficient direct preference optimization (Rafailov et al., 2024; Xu et al., 2024; Lee et al., 2024; Zhong et al., 2024), reference model free preference alignment (Meng et al., 2024; Hong et al., 2024b), generalized RLHF (Azar et al., 2024; Munos et al., 2023), safe RLHF (Dai et al., 2023), group preference learning (Zhao et al., 2023; Chakraborty et al., 2024), and theory or understanding of RLHF (Zhu et al., 2023a; Shen et al., 2024; Xiong et al., 2024; Wang et al., 2023; Kirk et al., 2023). In this work, we consider DPO (Rafailov et al., 2024) which has been used in training many popular open-source LLMs (Abdin et al., 2024; Dubey et al., 2024).

**SFT.** Another important step before using a pre-trained LLM in downstream applications is SFT (Howard & Ruder, 2018; Devlin, 2018; Wei et al., 2021; Zhu et al., 2023b; Zhang et al., 2023b). In recent years, there have been a large body of work on efficient LLM SFT; see, e.g., zeroth-order fine-tuning (Malladi et al., 2023a), quantized fine-tuning (Kim et al., 2024; Li et al., 2023b), parameter-efficient fine-tuning (Chen et al., 2023a; Zhang et al., 2023a; Shi & Lipani, 2023; Chen et al., 2023b; Nikdan et al., 2024), truthful fine-tuning (Tian et al., 2023), robust fine-tuning (Tian et al., 2024), SFT

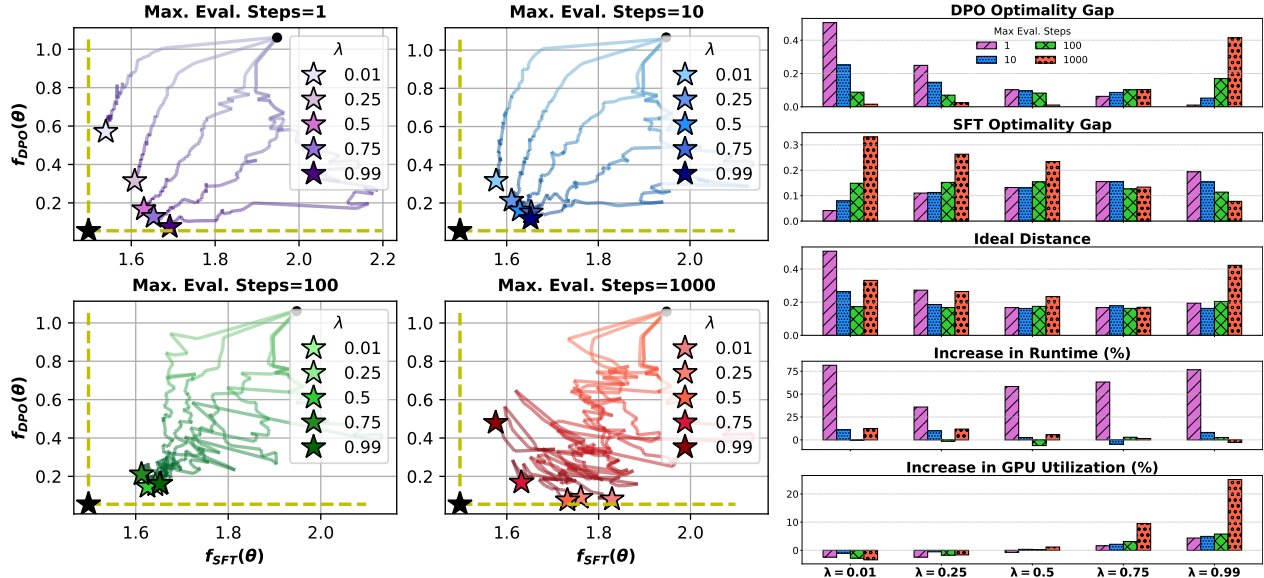


Figure 4: Comparison of different choices of evaluation steps for MAXRIGHT with Pythia-1b model.

with data selection (Lu et al., 2023; Kang et al., 2024; Zhao et al., 2024), self-play fine-tuning (Chen et al., 2024) and understanding of LLM fine-tuning (Malladi et al., 2023b).

**Sequential RLHF and SFT Issues.** Given the importance of both RLHF and SFT in LLM post-training, they are implemented as a sequential recipe (one after the other) on a pre-trained LLM. However, recent studies show that this either hinders the alignment performance (Qi et al., 2023), or fine-tuning performance (Ouyang et al., 2022), depending on the order of applying RLHF and SFT.

**Trade-off in RLHF and SFT.** Several methods have been proposed to reconcile RLHF and SFT in post training. One line of work attempt to remove a separate RLHF phase by adding regularization to SFT objective (Hong et al., 2024a), reformulation of SFT objective (Hua et al., 2024), and joint training using demonstrations and RLHF (Li et al., 2024). However, these methods restrict the use of different datasets for RLHF and SFT. Adaptive model averaging (AMA) (Lin et al., 2023) optimizes RLHF and SFT separately to balance objectives, but the original AMA is computationally expensive, requiring three sets of model parameters. While a memory-efficient AMA variant exists, its reliance on imitation learning weakens ties to the original objectives, and the relationship between AMA weights and optimal trade-offs remains unclear. Another line of work (Yang et al., 2024; Guo et al., 2024) propose to control deferent preferences in RLHF and SFT (independently) by post-training using data modified with prompt that encodes different preferences. In this work, the focus is on the trade-off between RLHF and SFT, and does not require modifications on the existing RLHF and SFT datasets.

## 6. Experiments

In this section we compare the proposed methods with some existing baselines, in terms of their Pareto-front performance and resource usage such as computation time and memory utilization.

### 6.1. Experimental setup

In this section, we introduce models, datasets, baselines, and evaluation metrics used to evaluate our proposed methods. Additional

experiment details are provided in Appendix D.

**Models.** We employ two architectures. The first is PYTHIA-1B<sup>1</sup>, a widely used model balancing computational efficiency and performance. Despite not being designed for downstream tasks, it matches or exceeds models like OPT and GPT-Neo of similar size. We use it to assess optimization dynamics, performance trade-offs, and resource usage of proposed methods. The second is LLAMA3-8B<sup>2</sup>, a larger model suited for fine-tuning and downstream real-world tasks. Both models are fine-tuned using Low-Rank Adaptation (LoRA) (Hu et al., 2021).

**Datasets.** For the DPO dataset, we use the DAHOAS/RM-HH-RLHF dataset, which contains human feedback data designed to align models to human preference. For the SFT phase, we use the VICGALLE/ALPACA-GPT4 dataset, which consists of English instruction-following data generated by GPT-4 using Alpaca prompts, designed for fine-tuning LLMs.

**Baseline Methods.** Comparing the performance of ALRIGHT and MAXRIGHT, we use the following baselines: Mix of DPO and SFT (‘Mix’), which simultaneously optimizes both DPO and SFT objectives by optimizing a convex combination of the objectives, and Sequential DPO and SFT (‘Sequential’), where DPO and SFT objectives are optimized one after the other.

**Evaluation Metrics.** To assess the performance of each method with respect to the DPO and SFT objectives, we utilize several evaluation metrics. For evaluating the DPO objective, we measure the **optimality gap** as  $f_{\text{DPO}}(\theta) - f_{\text{DPO}}^*$ , where  $f_{\text{DPO}}^*$  is approximated by independently optimizing the DPO objective for the same number of iterations as used for the baselines and proposed methods. The optimality gap for the SFT objective is similarly defined using the optimal value  $f_{\text{SFT}}^*$ , obtained by separately optimizing the SFT objective. To evaluate overall performance, we use the **ideal distance** metric, which represents the Euclidean distance

<sup>1</sup><https://huggingface.co/ElleutherAI/pythia-1b>

<sup>2</sup><https://huggingface.co/meta-llama/Meta-Llama-3-8B>

Table 1: Comparison of Win rate and MMLU (1-shot) for different methods using LLAMA3-8B.

| $\lambda/(T_{\text{SFT}}, T_{\text{DPO}})$ | MMLU (1-shot) (%) |              |              | Win rate (%) |              |              |
|--|-------------------|--------------|--------------|--------------|--------------|--------------|
|  | 0.25/(3, 1)       | 0.5/(2, 2)   | 0.75/(1, 3)  | 0.25/(3, 1)  | 0.5/(2, 2)   | 0.75/(1, 3)  |
| Sequential                                 | 73.18             | 72.80        | 72.68        | 57.19        | 65.62        | 59.38        |
| Mix  | 73.45             | 73.40        | 72.29        | 81.88        | 84.22        | <b>88.42</b> |
| ALRIGHT                                    | <b>74.66</b>      | 72.65        | <b>75.50</b> | <b>88.28</b> | 85.78        | 87.34        |
| MAXRIGHT                                   | 72.35             | <b>73.42</b> | 74.24        | 86.56        | <b>86.09</b> | 83.75        |

between the final iterate produced by the method and the point corresponding to optimal values for both DPO and SFT objectives:  $\sqrt{(f_{\text{DPO}}(\theta) - f_{\text{DPO}}^*)^2 + (f_{\text{SFT}}(\theta) - f_{\text{SFT}}^*)^2}$ . For resource efficiency, we compare the **percentage increase in runtime** relative to the corresponding sequential implementation, e.g., the percentage runtime increase of Alternating DPO and SFT with  $\lambda = 0.01$  compared to Sequential DPO and SFT with  $(T_{\text{DPO}}, T_{\text{SFT}}) = (1, 5)$ . Additionally, we compute the **percentage increase in GPU utilization** for each method relative to the baselines. Further details on these metrics are provided in Appendix D due to space constraints. Furthermore, for evaluating the real-world performance of proposed methods compared to baselines, we use the following benchmarks: **MMLU**(Hendrycks et al., 2020), a benchmark with multiple-choice questions across 57 diverse tasks; **Win rate**, which is calculated as the proportion of times a model’s response is preferred by an evaluator over a baseline in head-to-head comparisons. For this purpose, we use ALPACAEVAL(Li et al., 2023a) framework with GPT-4-TURBO as the evaluator and DAHOAS/RM-HH-RLHF test data as the baseline.

## 6.2. Experiment results

In this section, we illustrate and discuss the empirical results that compare the proposed methods with the baselines.

**ALRIGHT provides better control over the trade-off compared to Sequential.** As shown in the top left plot of Figure 3, the optimization trajectories for DPO followed by SFT illustrate that the set of final models produced by ALRIGHT, for various values of  $\lambda$ , is more evenly distributed in the objective space. This distribution forms a Pareto front, indicating that no model is strictly worse than another with respect to both objectives. Moreover, the spread of these models is comparable to that of the Mix method. In contrast, Sequential tends to produce models that are biased towards the SFT objective, even when  $T_{\text{DPO}}$  is significantly larger than  $T_{\text{SFT}}$  (e.g.,  $(T_{\text{DPO}}, T_{\text{SFT}}) = (5, 1)$ ).

**MAXRIGHT achieves near-ideal performance compared to other methods.** As illustrated in the top left plot of Figure 3, the optimization trajectories for DPO followed by SFT show that the set of final models produced by MAXRIGHT, for different values of  $\lambda$ , converge closer to the ideal point compared to other methods. This behavior is further supported by the Ideal Distance comparison in the right plot of Figure 3, where MAXRIGHT consistently achieves the best ideal distance performance across all  $\lambda$  values. We attribute this advantage to the adaptive nature of MAXRIGHT, which dynamically selects the objective to update based on performance, rather than adhering to a fixed schedule like ALRIGHT. This adaptability is particularly beneficial in heavily over-parameterized settings, where models have the capacity to approach ideal performance.

**ALRIGHT and MAXRIGHT require minimal additional resources compared to Sequential and significantly lower than Mix.** As shown in Figure 3 (right, Increase in Runtime (%) and Increase in GPU Utilization (%)), the additional computational resources required by different implementations of ALRIGHT and MAXRIGHT are minimal (or even negative) relative to their Sequential counterparts. In contrast, Mix incurs substantial additional resource usage, with increases of over 50% in runtime and more than 35% in GPU utilization, despite achieving similar performance metrics to ALRIGHT and MAXRIGHT.

**Effect of maximum evaluation step for memory-efficient MAXRIGHT.** Figure 4 illustrates the influence of maximum evaluation step choices in memory efficient MAXRIGHT on optimization trajectories and resource usage. For low values (e.g., 1), the algorithm closely follows the trade-off determined by  $\lambda$ , keeping the solutions concentrated near the ideal point (e.g., compared to ALRIGHT), but incurs high runtime due to frequent evaluations. In contrast, high values (e.g., 1000) cause significant oscillations in the objective space, failing to maintain the desired trade-off and resulting in increased GPU utilization from excessive SFT updates. The aforementioned oscillation leads to poor ideal distance performance as the model drifts away from the ideal point.

**ALRIGHT and MAXRIGHT significantly outperform Sequential on real-world tasks with minimal additional resources.** Table 1 presents a performance comparison of Sequential, Mix, ALRIGHT, and MAXRIGHT using the MMLU benchmark and win rate. ALRIGHT and MAXRIGHT consistently surpass the baselines on the MMLU benchmark and achieve a significantly higher win rate than Sequential across all  $\lambda$  values considered. On both evaluation metrics, either ALRIGHT or MAXRIGHT performs on par with or better than Mix. Furthermore, Figure 8 in Appendix D shows that ALRIGHT and MAXRIGHT require minimal additional resources, while Mix incurs significantly higher resource usage (up to 58% increase in runtime and 7% increase in GPU utilization).

## 7. Conclusions and Discussion

In this paper, we have shown both theoretically and empirically that the widely adopted sequential approach to post-training LLMs with RLHF and SFT is sub-optimal, as the model gradually forgets the effects of the initial stage during the second stage of training. Our proposed ALRIGHT and MAXRIGHT methods address this issue, with ALRIGHT providing theoretical convergence guarantees and MAXRIGHT demonstrating strong empirical performance. Notably, this improvement is achieved with minimal additional computational cost, making these methods practical and efficient alternatives for enhancing both the performance and preference alignment of LLMs.



## Impact Statement

This paper presents work whose goal is to advance the field of Machine Learning. There are many potential societal consequences of our work, none of which we feel must be specifically highlighted here.

## References

- Abdin, M., Jacobs, S. A., Awan, A. A., Aneja, J., Awadallah, A., Awadalla, H., Bach, N., Bahree, A., Bakhtiari, A., Behl, H., et al. Phi-3 technical report: A highly capable language model locally on your phone. *arXiv preprint arXiv:2404.14219*, 2024.
- Achiam, J., Adler, S., Agarwal, S., Ahmad, L., Akkaya, I., Aleman, F. L., Almeida, D., Altenschmidt, J., Altman, S., Anadkat, S., et al. Gpt-4 technical report. *arXiv preprint arXiv:2303.08774*, 2023.
- Azar, M. G., Guo, Z. D., Piot, B., Munos, R., Rowland, M., Valko, M., and Calandriello, D. A general theoretical paradigm to understand learning from human preferences. In *International Conference on Artificial Intelligence and Statistics*, pp. 4447–4455. PMLR, 2024.
- Bai, Y., Jones, A., Ndousse, K., Askell, A., Chen, A., DasSarma, N., Drain, D., Fort, S., Ganguli, D., Henighan, T., et al. Training a helpful and harmless assistant with reinforcement learning from human feedback. *arXiv preprint arXiv:2204.05862*, 2022a.
- Bai, Y., Kadavath, S., Kundu, S., Askell, A., Kernion, J., Jones, A., Chen, A., Goldie, A., Mirhoseini, A., McKinnon, C., et al. Constitutional ai: Harmlessness from ai feedback. *arXiv preprint arXiv:2212.08073*, 2022b.
- Chakraborty, S., Qiu, J., Yuan, H., Koppel, A., Huang, F., Manocha, D., Bedi, A. S., and Wang, M. Maxmin-rlhf: Towards equitable alignment of large language models with diverse human preferences. *arXiv preprint arXiv:2402.08925*, 2024.
- Chen, J., Zhang, A., Shi, X., Li, M., Smola, A., and Yang, D. Parameter-efficient fine-tuning design spaces. *arXiv preprint arXiv:2301.01821*, 2023a.
- Chen, Y., Qian, S., Tang, H., Lai, X., Liu, Z., Han, S., and Jia, J. Longlora: Efficient fine-tuning of long-context large language models. *arXiv preprint arXiv:2309.12307*, 2023b.
- Chen, Z., Deng, Y., Yuan, H., Ji, K., and Gu, Q. Self-play fine-tuning converts weak language models to strong language models. *arXiv preprint arXiv:2401.01335*, 2024.
- Christiano, P. F., Leike, J., Brown, T., Martic, M., Legg, S., and Amodei, D. Deep reinforcement learning from human preferences. *Advances in neural information processing systems*, 30, 2017.
- Dai, J., Pan, X., Sun, R., Ji, J., Xu, X., Liu, M., Wang, Y., and Yang, Y. Safe rlhf: Safe reinforcement learning from human feedback. *arXiv preprint arXiv:2310.12773*, 2023.
- Devlin, J. Bert: Pre-training of deep bidirectional transformers for language understanding. *arXiv preprint arXiv:1810.04805*, 2018.
- Ding, M., Ji, K., Wang, D., and Xu, J. Understanding forgetting in continual learning with linear regression. *arXiv preprint arXiv:2405.17583*, 2024.
- Dubey, A., Jauhri, A., Pandey, A., Kadian, A., Al-Dahle, A., Letman, A., Mathur, A., Schelten, A., Yang, A., Fan, A., et al. The llama 3 herd of models. *arXiv preprint arXiv:2407.21783*, 2024.
- Fang, Q., Guo, S., Zhou, Y., Ma, Z., Zhang, S., and Feng, Y. Llama-omni: Seamless speech interaction with large language models. *arXiv preprint arXiv:2409.06666*, 2024. URL <https://huggingface.co/ICTNLP/Llama-3.1-8B-Omni>.
- Guo, Y., Cui, G., Yuan, L., Ding, N., Sun, Z., Sun, B., Chen, H., Xie, R., Zhou, J., Lin, Y., et al. Controllable preference optimization: Toward controllable multi-objective alignment. *arXiv preprint arXiv:2402.19085*, 2024.
- Hendrycks, D., Burns, C., Basart, S., Zou, A., Mazeika, M., Song, D., and Steinhardt, J. Measuring massive multitask language understanding. *arXiv preprint arXiv:2009.03300*, 2020.
- Hong, J., Lee, N., and Thorne, J. Orpo: Monolithic preference optimization without reference model. *arXiv preprint arXiv:2403.07691*, 2(4):5, 2024a.
- Hong, J., Lee, N., and Thorne, J. Reference-free monolithic preference optimization with odds ratio. *arXiv e-prints*, pp. arXiv–2403, 2024b.
- Howard, J. and Ruder, S. Universal language model fine-tuning for text classification. *arXiv preprint arXiv:1801.06146*, 2018.
- Hu, E. J., Shen, Y., Wallis, P., Allen-Zhu, Z., Li, Y., Wang, S., Wang, L., and Chen, W. Lora: Low-rank adaptation of large language models. *arXiv preprint arXiv:2106.09685*, 2021.
- Hu, J., Wu, X., Wang, W., Xianyu, Zhang, D., and Cao, Y. Openrlhf: An easy-to-use, scalable and high-performance rlhf framework. *arXiv preprint arXiv:2405.11143*, 2024.
- Hua, E., Qi, B., Zhang, K., Yu, Y., Ding, N., Lv, X., Tian, K., and Zhou, B. Intuitive fine-tuning: Towards unifying sft and rlhf into a single process. *arXiv preprint arXiv:2405.11870*, 2024.
- Kang, F., Just, H. A., Sun, Y., Jahagirdar, H., Zhang, Y., Du, R., Sahu, A. K., and Jia, R. Get more for less: Principled data selection for warming up fine-tuning in llms. *arXiv preprint arXiv:2405.02774*, 2024.
- Kim, J., Lee, J. H., Kim, S., Park, J., Yoo, K. M., Kwon, S. J., and Lee, D. Memory-efficient fine-tuning of compressed large language models via sub-4-bit integer quantization. *Advances in Neural Information Processing Systems*, 36, 2024.
- Kirk, R., Mediratta, I., Nalmpantis, C., Luketina, J., Hambro, E., Grefenstette, E., and Raileanu, R. Understanding the effects of rlhf on llm generalisation and diversity. *arXiv preprint arXiv:2310.06452*, 2023.
- Lee, A., Bai, X., Pres, I., Wattenberg, M., Kummerfeld, J. K., and Mihalcea, R. A mechanistic understanding of alignment algorithms: A case study on dpo and toxicity. *arXiv preprint arXiv:2401.01967*, 2024.

- Li, C., Zeng, S., Liao, Z., Li, J., Kang, D., Garcia, A., and Hong, M. Joint demonstration and preference learning improves policy alignment with human feedback. *arXiv preprint arXiv:2406.06874*, 2024.
- Li, X., Zhang, T., Dubois, Y., Taori, R., Gulrajani, I., Guestrin, C., Liang, P., and Hashimoto, T. B. AlpacaEval: An automatic evaluator of instruction-following models. [https://github.com/tatsu-lab/alpaca\\_eval](https://github.com/tatsu-lab/alpaca_eval), 5 2023a.
- Li, Y., Yu, Y., Liang, C., He, P., Karampatziakis, N., Chen, W., and Zhao, T. Loftq: Lora-fine-tuning-aware quantization for large language models. *arXiv preprint arXiv:2310.08659*, 2023b.
- Lin, Y., Tan, L., Lin, H., Zheng, Z., Pi, R., Zhang, J., Diao, S., Wang, H., Zhao, H., Yao, Y., et al. Speciality vs generality: An empirical study on catastrophic forgetting in fine-tuning foundation models. *arXiv preprint arXiv:2309.06256*, 2023.
- Lu, K., Yuan, H., Yuan, Z., Lin, R., Lin, J., Tan, C., Zhou, C., and Zhou, J. # instag: Instruction tagging for analyzing supervised fine-tuning of large language models. In *The Twelfth International Conference on Learning Representations*, 2023.
- Malladi, S., Gao, T., Nichani, E., Damian, A., Lee, J. D., Chen, D., and Arora, S. Fine-tuning language models with just forward passes. *Advances in Neural Information Processing Systems*, 36:53038–53075, 2023a.
- Malladi, S., Wettig, A., Yu, D., Chen, D., and Arora, S. A kernel-based view of language model fine-tuning. In *International Conference on Machine Learning*, pp. 23610–23641. PMLR, 2023b.
- Meng, Y., Xia, M., and Chen, D. Simpo: Simple preference optimization with a reference-free reward. *arXiv preprint arXiv:2405.14734*, 2024.
- Miettinen, K. *Nonlinear multiobjective optimization*, volume 12. Springer Science & Business Media, 1999.
- Munos, R., Valko, M., Calandriello, D., Azar, M. G., Rowland, M., Guo, Z. D., Tang, Y., Geist, M., Mesnard, T., Michi, A., et al. Nash learning from human feedback. *arXiv preprint arXiv:2312.00886*, 2023.
- Nikdan, M., Tabesh, S., and Alistarh, D. Rosa: Accurate parameter-efficient fine-tuning via robust adaptation. *arXiv preprint arXiv:2401.04679*, 2024.
- OpenAI. Chatgpt: Optimizing language models for dialogue, November 2022. URL <https://openai.com/blog/chatgpt/>. Accessed: 2024-08-28.
- Orabona, F. Last iterate of sgd converges even in unbounded domains, 2020. URL <https://parameterfree.com/2020/08/07/last-iterate-of-sgd-converges-even-in-unbounded-domains/>. Accessed: 2024-09-10.
- Ouyang, L., Wu, J., Jiang, X., Almeida, D., Wainwright, C., Mishkin, P., Zhang, C., Agarwal, S., Slama, K., Ray, A., et al. Training language models to follow instructions with human feedback. *Advances in neural information processing systems*, 35:27730–27744, 2022.
- Qi, X., Zeng, Y., Xie, T., Chen, P.-Y., Jia, R., Mittal, P., and Henderson, P. Fine-tuning aligned language models compromises safety, even when users do not intend to! *arXiv preprint arXiv:2310.03693*, 2023.
- Rafailov, R., Sharma, A., Mitchell, E., Manning, C. D., Ermon, S., and Finn, C. Direct preference optimization: Your language model is secretly a reward model. *Advances in Neural Information Processing Systems*, 36, 2024.
- Rockafellar, R. T. Convex analysis, 1970.
- Roziere, B., Gehring, J., Gloeckle, F., Sootla, S., Gat, I., Tan, X. E., Adi, Y., Liu, J., Sauvestre, R., Remez, T., et al. Code llama: Open foundation models for code. *arXiv preprint arXiv:2308.12950*, 2023.
- Shen, H., Yang, Z., and Chen, T. Principled penalty-based methods for bilevel reinforcement learning and rlhf. *arXiv preprint arXiv:2402.06886*, 2024.
- Shi, Z. and Lipani, A. Dept: Decomposed prompt tuning for parameter-efficient fine-tuning. *arXiv preprint arXiv:2309.05173*, 2023.
- Sun, Z., Shen, Y., Zhou, Q., Zhang, H., Chen, Z., Cox, D., Yang, Y., and Gan, C. Principle-driven self-alignment of language models from scratch with minimal human supervision. *Advances in Neural Information Processing Systems*, 36, 2024.
- Tang, Y., Tran, C., Li, X., Chen, P.-J., Goyal, N., Chaudhary, V., Gu, J., and Fan, A. Multilingual translation with extensible multilingual pretraining and finetuning. *arXiv preprint arXiv:2008.00401*, 2020. URL <https://huggingface.co/SnypzZz/Llama2-13b-Language-translate>.
- Tian, J., Liu, Y.-C., Smith, J. S., and Kira, Z. Fast trainable projection for robust fine-tuning. *Advances in Neural Information Processing Systems*, 36, 2024.
- Tian, K., Mitchell, E., Yao, H., Manning, C. D., and Finn, C. Fine-tuning language models for factuality. *arXiv preprint arXiv:2311.08401*, 2023.
- Wang, Y., Liu, Q., and Jin, C. Is rlhf more difficult than standard rl? a theoretical perspective. *Advances in Neural Information Processing Systems*, 36:76006–76032, 2023.
- Wei, J., Bosma, M., Zhao, V. Y., Guu, K., Yu, A. W., Lester, B., Du, N., Dai, A. M., and Le, Q. V. Finetuned language models are zero-shot learners. *arXiv preprint arXiv:2109.01652*, 2021.
- Xiong, W., Dong, H., Ye, C., Wang, Z., Zhong, H., Ji, H., Jiang, N., and Zhang, T. Iterative preference learning from human feedback: Bridging theory and practice for rlhf under kl-constraint. In *Forty-first International Conference on Machine Learning*, 2024.
- Xu, S., Fu, W., Gao, J., Ye, W., Liu, W., Mei, Z., Wang, G., Yu, C., and Wu, Y. Is dpo superior to ppo for llm alignment? a comprehensive study. *arXiv preprint arXiv:2404.10719*, 2024.
- Yang, R., Pan, X., Luo, F., Qiu, S., Zhong, H., Yu, D., and Chen, J. Rewards-in-context: Multi-objective alignment of foundation models with dynamic preference adjustment. *arXiv preprint arXiv:2402.10207*, 2024.

- Zhang, Q., Chen, M., Bukharin, A., Karampatziakis, N., He, P., Cheng, Y., Chen, W., and Zhao, T. Adalora: Adaptive budget allocation for parameter-efficient fine-tuning. *arXiv preprint arXiv:2303.10512*, 2023a.
- Zhang, S., Dong, L., Li, X., Zhang, S., Sun, X., Wang, S., Li, J., Hu, R., Zhang, T., Wu, F., et al. Instruction tuning for large language models: A survey. *arXiv preprint arXiv:2308.10792*, 2023b.
- Zhao, H., Andriushchenko, M., Croce, F., and Flammarion, N. Long is more for alignment: A simple but tough-to-beat baseline for instruction fine-tuning. *arXiv preprint arXiv:2402.04833*, 2024.
- Zhao, S., Dang, J., and Grover, A. Group preference optimization: Few-shot alignment of large language models. *arXiv preprint arXiv:2310.11523*, 2023.
- Zhong, H., Feng, G., Xiong, W., Zhao, L., He, D., Bian, J., and Wang, L. Dpo meets ppo: Reinforced token optimization for rlhf. *arXiv preprint arXiv:2404.18922*, 2024.
- Zhu, B., Jordan, M., and Jiao, J. Principled reinforcement learning with human feedback from pairwise or k-wise comparisons. In *International Conference on Machine Learning*, pp. 43037–43067. PMLR, 2023a.
- Zhu, D., Chen, J., Shen, X., Li, X., and Elhoseiny, M. Minigt-4: Enhancing vision-language understanding with advanced large language models. *arXiv preprint arXiv:2304.10592*, 2023b.

## Supplementary Material for “Mitigating Forgetting in LLM Supervised Fine-Tuning and Preference Learning”

### A. Proofs for Theoretical Results

In this section, we provide the proofs for the main theoretical results of the paper, Theorems 3.3 and 4.1. The proof is organized as follows: In Appendix A.1, we establish some fundamental claims regarding the problem setup, such as the convexity of the objectives and the boundedness of the second moment of the stochastic gradients. Then, in Appendix A.2, we prove the lower bound stated in Theorem 3.3 along with several supporting lemmas. Finally, in Appendix A.3, we prove the upper bound stated in Theorem 4.1, accompanied by additional supporting lemmas.

For conciseness, in this section we omit the subscripts DPO and SFT of the input  $x$ , but whether  $x$  belongs to  $\mathcal{D}_{\text{DPO}}$  or  $\mathcal{D}_{\text{SFT}}$  can be inferred from the context. Furthermore, for brevity, we denote the averaging over the datasets  $\frac{1}{N_1} \sum_{x, y_w, y_\ell \in \mathcal{D}_{\text{DPO}}}$  and  $\frac{1}{N_2} \sum_{x, y \in \mathcal{D}_{\text{SFT}}}$  by  $\mathbb{E}_{x, y_w, y_\ell \sim \mathcal{D}_{\text{DPO}}}$  and  $\mathbb{E}_{x, y \sim \mathcal{D}_{\text{SFT}}}$ , respectively.

#### A.1. Basic claims on the problem setup

Before going to the proofs of the main results, we can have the following basic claims on the problem setup.

**Proposition A.1** (Bounded second moment of stochastic gradient). *For all  $\theta \in \Theta$ , there exist  $M_1, M_2 > 0$  such that*

$$\mathbb{E}_{x, y_w, y_\ell \sim \mathcal{D}_{\text{DPO}}} [\|g_{\text{DPO}}(\theta; x, y_w, y_\ell)\|^2] \leq M_1^2, \quad (20)$$

$$\mathbb{E}_{x, y \sim \mathcal{D}_{\text{SFT}}} [\|g_{\text{SFT}}(\theta; x, y)\|^2] \leq M_2^2. \quad (21)$$

*Proof.* Considering  $g_{\text{DPO}}$ , we can first simplify  $h_\beta$  defined in (3) under softmax parameterization of  $\pi_\theta$  and  $\pi_{\text{ref}}$  as

$$\begin{aligned} h_\beta(\theta; x, y_w, y_\ell) &= \beta \log \left( \frac{\pi_\theta(y_w | x)}{\pi_{\text{ref}}(y_w | x)} \right) - \beta \log \left( \frac{\pi_\theta(y_\ell | x)}{\pi_{\text{ref}}(y_\ell | x)} \right) \\ &= \beta(\theta - \theta_{\text{ref}})^\top (\phi_{y_w, x} - \phi_{y_\ell, x}). \end{aligned} \quad (22)$$

Then we can simplify  $g_{\text{DPO}}$  as

$$\begin{aligned} g_{\text{DPO}}(\theta; x, y_w, y_\ell) &= -(1 - \sigma(h_\beta(\theta; x, y_w, y_\ell, \pi_{\text{ref}}))) \nabla_\theta h_\beta(\theta; x, y_w, y_\ell, \pi_{\text{ref}}) \\ &= -\beta(1 - \sigma(\beta(\theta - \theta_{\text{ref}})^\top (\phi_{y_w, x} - \phi_{y_\ell, x}))) (\phi_{y_w, x} - \phi_{y_\ell, x}). \end{aligned} \quad (23)$$

We can then bound the norm of  $g_{\text{DPO}}$  as

$$\begin{aligned} \|g_{\text{DPO}}(\theta; x, y_w, y_\ell)\|^2 &= \beta^2(1 - \sigma(\beta(\theta - \theta_{\text{ref}})^\top (\phi_{y_w, x} - \phi_{y_\ell, x})))^2 \|\phi_{y_w, x} - \phi_{y_\ell, x}\|^2 \\ &\leq \beta^2 \|\phi_{y_w, x} - \phi_{y_\ell, x}\|^2 \\ &\leq 4\beta^2 \Phi^2 =: M_1, \end{aligned} \quad (24)$$

where the first inequality is due to the fact that  $0 \leq \sigma(z) \leq 1$  for all  $z \in \mathbb{R}$ , second inequality is due to Cauchy-Schwarz inequality and Assumption 3.2. Taking expectation (average) over the dataset  $\mathcal{D}_{\text{DPO}}$  in (24) proves the first part of Proposition A.1. For proving the second part of the proposition, we start by simplifying the gradient of  $\pi_\theta$  under softmax-parameteriation, given by

$$\begin{aligned} \nabla_\theta \pi_\theta(y | x) &= \nabla_\theta \frac{\exp(\theta^\top \phi_{y, x})}{\sum_{y' \in \mathcal{Y}} \exp(\theta^\top \phi_{y', x})} \\ &= \frac{\exp(\theta^\top \phi_{y, x}) \sum_{y' \in \mathcal{Y}} \exp(\theta^\top \phi_{y', x}) \phi_{y, x} - \exp(\theta^\top \phi_{y, x}) \sum_{y' \in \mathcal{Y}} \exp(\theta^\top \phi_{y', x}) \phi_{y', x}}{\left( \sum_{y' \in \mathcal{Y}} \exp(\theta^\top \phi_{y', x}) \right)^2} \\ &= (\phi_{y, x} - \bar{\phi}_x(\theta)) \pi_\theta(y | x), \end{aligned} \quad (25)$$

where

$$\bar{\phi}_x(\theta) := \frac{\sum_{y' \in \mathcal{Y}} \phi_{y', x} \exp(\theta^\top \phi_{y', x})}{\sum_{y' \in \mathcal{Y}} \exp(\theta^\top \phi_{y', x})}. \quad (26)$$

Then we can simplify  $g_{\text{SFT}}$  as

$$\begin{aligned} g_{\text{SFT}}(\theta; x, y) &= -\frac{\nabla_\theta \pi_\theta(y | x)}{\pi_\theta(y | x)} \\ &= -(\phi_{y, x} - \bar{\phi}_x(\theta)). \end{aligned} \quad (27)$$

We can then bound the norm of  $g_{\text{SFT}}$  as

$$\begin{aligned} \|g_{\text{SFT}}(\theta; x, y)\|^2 &= \|\phi_{y,x} - \bar{\phi}_x(\theta)\|^2 \\ &\leq 4\Phi^2 =: M_2, \end{aligned} \quad (28)$$

where the inequality is due to the Cauchy-Schwarz inequality and Jensen's inequality. Taking expectation (average) over the dataset  $\mathcal{D}_{\text{SFT}}$  in (28) proves the second part of Proposition A.1.  $\square$

**Proposition A.2** (Convexity of objectives). *Under Assumption 3.2, the objectives  $f_{\text{DPO}}$  and  $f_{\text{SFT}}$  (defined in (1) and (4), respectively) are convex.*

*Proof.* The goal of the proof is to show the Hessians of the objectives  $f_{\text{DPO}}$  and  $f_{\text{SFT}}$  are semi-positive definite, under Assumption 3.2 and LLMs (both trainable and reference) modeled using softmax parameterization. First, considering  $f_{\text{DPO}}$ , we can have

$$\begin{aligned} \nabla_{\theta} g_{\text{DPO}}(\theta; x, y_w, y_{\ell}) &= -\nabla_{\theta} \beta (1 - \sigma(\beta(\theta - \theta_{\text{ref}})^{\top} (\phi_{y_w,x} - \phi_{y_{\ell},x}))) (\phi_{y_w,x} - \phi_{y_{\ell},x}) \\ &= \beta^2 \sigma(h_{\beta}(\theta; x, y_w, y_{\ell})) (\phi_{y_w,x} - \phi_{y_{\ell},x}) (\phi_{y_w,x} - \phi_{y_{\ell},x})^{\top} \succeq 0, \end{aligned} \quad (29)$$

where first equality is due to (23), and the semi-positive definiteness is due to the fact that  $\beta > 0$ ,  $0 \leq \sigma(z) \leq 1$  for all  $z \in \mathbb{R}$ , and  $(\phi_{y_w,x} - \phi_{y_{\ell},x}) (\phi_{y_w,x} - \phi_{y_{\ell},x})^{\top} \succeq 0$  for all  $\phi_{y_w,x}, \phi_{y_{\ell},x}$ . The convexity of  $f_{\text{DPO}}$  follows from the fact that

$$\nabla^2 f_{\text{DPO}}(\theta) = \mathbb{E}_{x, y_w, y_{\ell} \sim \mathcal{D}_{\text{DPO}}} [\nabla_{\theta} g_{\text{DPO}}(\theta; x, y_w, y_{\ell})]. \quad (30)$$

Similarly, we can compute  $\nabla_{\theta} g_{\text{SFT}}$  as

$$\begin{aligned} \nabla_{\theta} g_{\text{SFT}}(\theta; x, y) &= -\nabla_{\theta} (\phi_{y,x} - \bar{\phi}_x(\theta)) \\ &= \nabla_{\theta} \frac{\sum_{y' \in \mathcal{Y}} \phi_{y',x} \exp(\theta^{\top} \phi_{y',x})}{\sum_{y' \in \mathcal{Y}} \exp(\theta^{\top} \phi_{y',x})} \\ &= \sum_{y' \in \mathcal{Y}} \frac{\phi_{y',x} \phi_{y',x}^{\top} \exp(\theta^{\top} \phi_{y',x})}{\sum_{y' \in \mathcal{Y}} \exp(\theta^{\top} \phi_{y',x})} \\ &\quad - \left( \frac{\sum_{y' \in \mathcal{Y}} \phi_{y',x} \exp(\theta^{\top} \phi_{y',x})}{\sum_{y' \in \mathcal{Y}} \exp(\theta^{\top} \phi_{y',x})} \right) \left( \frac{\sum_{y' \in \mathcal{Y}} \phi_{y',x} \exp(\theta^{\top} \phi_{y',x})}{\sum_{y' \in \mathcal{Y}} \exp(\theta^{\top} \phi_{y',x})} \right)^{\top}, \end{aligned} \quad (31)$$

where the first equality is due to (27). To establish the semi-positivedefiniteness of  $\nabla_{\theta} g_{\text{SFT}}$ , consider any  $v$  with same dimension as  $\theta$ , and let  $p_{y,x} = \frac{\exp(\theta^{\top} \phi_{y,x})}{\sum_{y' \in \mathcal{Y}} \exp(\theta^{\top} \phi_{y',x})}$ . Note that  $p_{y,x} \geq 0$  for all  $x, y$ , and  $\sum_{y \in \mathcal{Y}} p_{y,x} = 1$  for all  $x$ . Then we can have

$$\begin{aligned} &v^{\top} \left( \sum_{y' \in \mathcal{Y}} \frac{\phi_{y',x} \phi_{y',x}^{\top} \exp(\theta^{\top} \phi_{y',x})}{\sum_{y' \in \mathcal{Y}} \exp(\theta^{\top} \phi_{y',x})} \right. \\ &\quad \left. - \left( \frac{\sum_{y' \in \mathcal{Y}} \phi_{y',x} \exp(\theta^{\top} \phi_{y',x})}{\sum_{y' \in \mathcal{Y}} \exp(\theta^{\top} \phi_{y',x})} \right) \left( \frac{\sum_{y' \in \mathcal{Y}} \phi_{y',x} \exp(\theta^{\top} \phi_{y',x})}{\sum_{y' \in \mathcal{Y}} \exp(\theta^{\top} \phi_{y',x})} \right)^{\top} \right) v \\ &= \sum_{y' \in \mathcal{Y}} (v^{\top} \phi_{y',x})^2 p_{y',x} - \left( \sum_{y' \in \mathcal{Y}} v^{\top} \phi_{y',x} p_{y',x} \right)^2 \geq 0, \end{aligned} \quad (32)$$

where the last inequality is due to Jensen's inequality. This suggests that  $\nabla_{\theta} g_{\text{SFT}}(\theta; x, y) \succeq 0$ , and the convexity of  $f_{\text{SFT}}$  follows from the fact that

$$\nabla^2 f_{\text{SFT}}(\theta) = \mathbb{E}_{x, y \sim \mathcal{D}_{\text{SFT}}} [\nabla_{\theta} g_{\text{SFT}}(\theta; x, y)]. \quad (33)$$

Note that when  $f_{\text{DPO}}$  and  $f_{\text{SFT}}$  are convex,  $f_{\text{Mix}, \lambda}$  is also convex for all  $\lambda \in [0, 1]$ .  $\square$

## A.2. Proof of Theorem 3.3

*Proof.* For deriving the lower bound given in 3.3, we consider the following problem setup that satisfies Assumption 3.2. Let  $\Theta$  be  $\mathbb{R}$ , and let  $\mathcal{D}_{\text{DPO}} = \{(x_1, y_w, y_{\ell})\}$  and  $\mathcal{D}_{\text{SFT}} = \{(x_2, y)\}$  and consider only two possible outputs exist (i.e. binary classification) such that we have the specification in Table 2. Note that the data point  $y'$  is not used in training explicitly, and it is specified to enable the calculation of the output of  $\pi_{\theta}$  with softmax parameterization in the SFT optimization phase. Based on this dataset, we can also define the dataset for

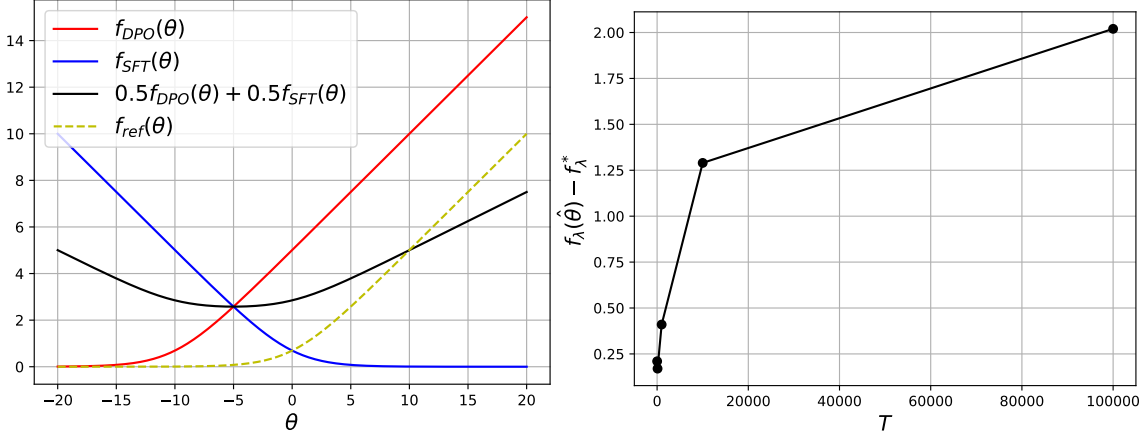


Figure 5: An Illustration of the example used for lower bound derivation in Theorem 3.3

Table 2: Data set specification for lower bound analysis example

| Input | Output       | Feature $\phi_{y,x}$ |
|-------|--------------|----------------------|
| $x_1$ | $y_w = 1$    | -1.0                 |
| $x_1$ | $y_\ell = 0$ | -0.5                 |
| $x_2$ | $y = 0$      | 1.0                  |
| $x_2$ | $y' = 1$     | 0.5                  |

reference policy objective as  $\mathcal{D}_{\text{ref}} = \{(x_1, y_w)\}$ , which has a similar optimization procedure as SFT. Before moving forward, we have to choose the reference policy  $\pi_{\text{ref}}$ , or equivalently  $\theta_{\text{ref}}$ . The objective to determine  $\theta_{\text{ref}}$  is given by

$$\theta_{\text{ref}} \in \underset{\theta}{\operatorname{argmin}} f_{\text{ref}}(\theta) := -\log \pi_{\theta}(y_w | x_1), \quad (34)$$

which is graphically illustrated in Figure 5. We choose  $\theta_{\text{ref}} = -5$  since this choice reasonably optimizes the objective.

With this problem setup and choice of  $\theta_{\text{ref}}$ , we can then derive the objectives and corresponding gradients using (1), (4), (23), and (27) as

$$f_{\text{DPO}}(\theta) = \log \left( 1 + c \frac{1 + \exp(\theta/2)}{1 + \exp(-\theta/2)} \right) \quad (35)$$

$$f_{\text{SFT}}(\theta) = \log(1 + \exp(-\theta/2)) \quad (36)$$

$$g_{\text{DPO}}(\theta) = \frac{1}{2} \cdot \frac{1}{1 + \exp(-(\theta/2 + 5))} \quad (37)$$

$$g_{\text{SFT}}(\theta) = -\frac{1}{2} \cdot \frac{1}{1 + \exp(\theta/2)}, \quad (38)$$

where  $c = \frac{1 + \exp(5)}{1 + \exp(-5)}$ . Choosing  $\lambda = 0.5$ , we can numerically find an upper bound to  $f_{\text{Mix},\lambda}^*$  such that  $f_{\text{Mix},\lambda}^* \leq \frac{1}{2} \log c^*$  where  $c^* = 173.78$ . With this, we can derive a lower bound to  $G_{\text{Mix},\lambda}(\theta)$  as

$$\begin{aligned} G_{\text{Mix},\lambda}(\theta) &= f_{\text{Mix},\lambda}(\theta) - f_{\text{Mix},\lambda}^* \\ &\geq \frac{1}{2} \cdot \log \left( 1 + c \frac{1 + \exp(\theta/2)}{1 + \exp(-\theta/2)} \right) + \frac{1}{2} \cdot \log(1 + \exp(-\theta/2)) - \frac{1}{2} \log c^* \\ &= \frac{1}{2} \log \left( \frac{1}{c^*} (1 + \exp(-\theta/2)) + \frac{c}{c^*} (1 + \exp(\theta/2)) \right). \end{aligned} \quad (39)$$

When  $\theta = 0$ , the right hand side of (39) approximately equals 0.256843. Since it is monotonically increasing for  $\theta \in [0, \infty)$ , we have  $G_{\text{Mix},\lambda}(\theta) \gtrsim 0.256843 = \Omega(1)$  when  $\theta \geq 0$ . Thus to prove the result, it is sufficient to show Algorithm 1 will generate a  $\hat{\theta}_{\text{Seq}}$  that is greater than 0.

We have the first stage iterates:

$$\theta_{t+1}^1 = \theta_t^1 - \alpha_t \frac{1}{1 + \exp(-\frac{\theta_t^1}{2} - 5)}, \quad \text{for } t = 1, \dots, T-1. \quad (40)$$

Using the first stage's last iterate as initial point, we have the second stage iterates:

$$\theta_{t+1}^{2,T} = \theta_t^{2,T} + \alpha_t \frac{1}{1 + \exp(\frac{\theta_t^{2,T}}{2})}, \text{ for } t = 1, \dots, T-1. \quad (41)$$

where  $\theta_1^{2,T} = \theta_T^1$  and the superscript  $T$  in  $\theta_t^{2,T}$  indicates the max iteration index in the first stage.

Without loss of generality, we initialize  $\theta_1^1 = 0$ . Then by (40) and (41), we have

$$\hat{\theta}_{\text{Seq}} = \theta_T^{2,T} = -\alpha_t \sum_{t=1}^{T-1} \frac{1}{1 + \exp(-\frac{\theta_t^1 + 10}{2})} + \alpha_t \sum_{t=1}^{T-1} \frac{1}{1 + \exp(\frac{\theta_t^{2,T}}{2})} \quad (42)$$

We first prove the following lemma.

**Lemma A.3.** *Given a positive constant  $c$  and a sequence  $\{\alpha_t\}$ , consider the iterates generated by*

$$\theta_{t+1} = \theta_t + \alpha_t \frac{1}{1 + \exp(c\theta_t)}, \quad \theta'_{t+1} = \theta'_t + \alpha_t \frac{1}{1 + \exp(c\theta'_t)} \quad (43)$$

If  $\theta_1 - \theta'_1 \geq 0$  and  $\frac{c\alpha_t}{4} \leq 1$  for any  $t$ , then we have

$$\theta_t - \theta'_t \geq (\theta_1 - \theta'_1) \prod_{i=1}^{t-1} \left(1 - \frac{c\alpha_i}{4}\right), \quad \forall t.$$

*Proof.* We prove the result by induction. Assume  $\theta_t - \theta'_t \geq 0$  for some  $t$ . We first have

$$\theta_{t+1} - \theta'_{t+1} = \theta_t - \theta'_t + \alpha_t \left( \frac{1}{1 + \exp(c\theta_t)} - \frac{1}{1 + \exp(c\theta'_t)} \right) \quad (44)$$

With  $\nabla_{\theta} \frac{1}{1 + \exp(c\theta)} = -c\sigma(-c\bar{\theta})(1 - \sigma(-c\bar{\theta}))$  where  $\sigma$  is the sigmoid function, using the mean value theorem in (44), we have for some  $\bar{\theta}_t$  in between  $\theta_t$  and  $\theta'_t$  that

$$\begin{aligned} \theta_{t+1} - \theta'_{t+1} &= \theta_t - \theta'_t - c\alpha_t \sigma(-c\bar{\theta}_t)(1 - \sigma(-c\bar{\theta}_t))(\theta_t - \theta'_t) \\ &\geq \theta_t - \theta'_t - \frac{1}{4}c\alpha_t(\theta_t - \theta'_t) \\ &= \left(1 - \frac{1}{4}c\alpha_t\right)(\theta_t - \theta'_t) \end{aligned}$$

where the inequality follows from  $\sigma(-c\bar{\theta}_t)(1 - \sigma(-c\bar{\theta}_t)) \leq \max_{x \in [0,1]} x(1-x) = \frac{1}{4}$  and the assumption that  $\theta_t - \theta'_t \geq 0$ . Since  $\theta_1 - \theta'_1 \geq 0$ , it follows from induction that  $\theta_t - \theta'_t \geq 0$  for any  $t$ . Then recursively applying the last inequality completes the proof.  $\square$

Now we consider (42). Rewriting (40) gives that  $\theta_t^1$  is generated by

$$-(\theta_{t+1}^1 + 10) = -(\theta_t^1 + 10) + \alpha_t \frac{1}{1 + \exp(-\frac{\theta_t^1 + 10}{2})}, \text{ for } t = 1, \dots, T-1,$$

and  $\theta_t^{2,T}$  is generated by (41). Thus  $\theta_t^{2,T}$  and  $-(\theta_t^1 + 10)$  are generated by (43) with  $c = 1/2$ . Assuming the step size  $\alpha_t$  is proper that  $\sum_{t=1}^{\infty} \alpha_t = \infty$ , then there always exists  $T^*$  that for  $T \geq T^*$ , we have  $\theta_T^1$  is small enough such that  $-(\theta_1^1 + 10) - \theta_1^{2,T} = -10 - \theta_T^1 \geq 0$ . If  $\alpha_t/8 \leq 1$ , we have Lemma A.3 holds for sequences  $\theta_t^{2,T}$  and  $-(\theta_{t+1}^1 + 10)$ , and we have

$$-(\theta_t^1 + 10) \geq \theta_t^{2,T} \Rightarrow \frac{1}{1 + \exp(\theta_t^{2,T}/2)} - \frac{1}{1 + \exp(-(\theta_t^1 + 10)/2)} \geq 0. \quad (45)$$

Using (45) in (42), we have  $\hat{\theta}_{\text{Seq}} \geq 0$ . This completes the proof.  $\square$

**Remark A.4.** We provide some intuition on why we can obtain this suboptimality result for the sequential method, how the proposed methods can overcome the suboptimality, and evidence for causes of suboptimality in real-world post training tasks:

**Cause of suboptimality.** The key idea behind the suboptimality result is constructing two conflicting objectives for DPO and SFT. To this end, we exploit the fact that DPO and SFT datasets can be diverse, and they can have inconsistencies in labelling. Specifically, in our lower bound analysis, we selected DPO and SFT inputs (by choosing the features  $\phi_{x,y}$ ) and corresponding labels  $y_w, y_\ell$ , and  $y$  such that the DPO and SFT objectives induced by these datasets conflict with each other (Table 2). Note that in this example both inputs and

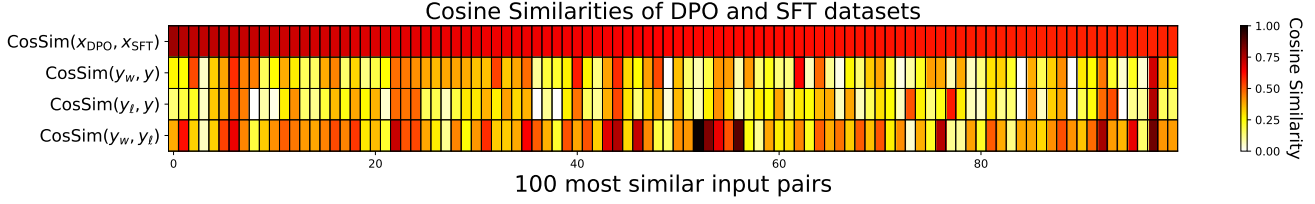


Figure 6: Visualization of data diversity and labeling inconsistencies in DPO (RM-HH-RLHF) and SFT (ALPACA-GPT4) datasets.

labels are different, thus there is no explicit labeling inconsistency. More severely conflicting DPO and SFT objectives can be constructed by fixing the input (and hence the corresponding feature  $\phi_{x,y}$ ) for both DPO and SFT datasets and assign conflicting labels to the chosen response for the DPO input and the target response for the SFT input. However, we used a more general example in our lower bound analysis, which shows that even when there is no explicit labeling inconsistency (e.g., when the input data for the two datasets are different), the sequential approach can still fail.

**How proposed methods can overcome suboptimality?** The strength of the proposed alternating approaches over the sequential approach is not its ability to explicitly correct any diversity in the datasets or inconsistency in labeling. Rather, it lies in their ability to navigate the loss landscape of both fine-tuning and alignment objectives, reasonably optimizing both. Given two (possibly conflicting) datasets and a pretrained LLM, our proposed methods can achieve a model that is most reasonably optimal for both SFT and alignment datasets, with a controllable trade-off between them.

**Data diversity and labeling inconsistency in real-world data.** We investigated the data diversity and labeling inconsistencies in our real-world experiments (e.g., Figures 3 and 7) using the datasets ALPACA-GPT4 for SFT and RM-HH-RLHF for DPO. Specifically, we visualized:

- cosine similarities between the closest input pairs  $(x_{\text{DPO}}^{(i)}, x_{\text{SFT}}^{(i)})$  from the two datasets;
- cosine similarities between chosen/rejected responses for the DPO input and the target response for the corresponding SFT input  $((y_w^{(i)}, y_\ell^{(i)})/(y_\ell^{(i)}, y^{(i)}))$ ; and,
- cosine similarities between chosen/rejected responses of the DPO input  $(y_w^{(i)}, y_\ell^{(i)})$ . Here, the superscript  $(i)$  denotes the ranking of the DPO-SFT input pair based on their similarity, which was measured at the token level.

The visualization is given in Figure 6. It can be observed that most DPO and SFT input pairs do not exhibit very strong cosine similarity (falling in the range of approximately 0.57–0.78). Observing the corresponding inputs, the similarity seems to come from mainly the sentence structure, rather than the underlying meaning. Thus, there is some inherent dissimilarity in the inputs themselves. Furthermore, for some similar input pairs  $(x_{\text{DPO}}^{(i)}, x_{\text{SFT}}^{(i)})$ , the corresponding  $(y_w^{(i)}, y_\ell^{(i)})$  similarity is close to zero, which might indicate a conflict in labeling. This suggests that there is some inconsistency in labeling in the real-world setup, although it is not as conclusive or adversarial as in the toy example used for the lower bound analysis. While here we use a token level comparison using cosine similarity, A deeper investigation into these data-level inconsistencies would be valuable, particularly in addressing them during data preprocessing or selection to enhance the optimization process.

### A.3. Proof of Theorem 4.1

In this section, we provide the proof for Theorem 4.1. First, we provide some useful results that will later be used in the main proof. For conciseness, we denote  $g_{\text{DPO}}(\theta_t; x^t, y_w^t, y_\ell^t)$  and  $g_{\text{SFT}}(\theta_t; x^t, y^t)$  by  $g_{\text{DPO},t}$  and  $g_{\text{SFT},t}$ , respectively.

**Lemma A.5** ((Rockafellar, 1970) Theorem 25.1 and Corollary 25.11). *Consider any convex differentiable function  $f$  and let  $\theta \in \Theta$ . Then, for any  $\theta' \in \Theta$ , we have*

$$f(\theta') \geq f(\theta) + \nabla f(\theta)^\top (\theta' - \theta). \quad (46)$$

**Lemma A.6** ((Orabona, 2020) Lemma 1.). *Let  $\{\eta_t\}_{t=1}^T$  be a non-increasing sequence of positive numbers and  $q_t \geq 0$  for all  $t = 1, \dots, T$ . Then*

$$n_T q_T \leq \frac{1}{T} \sum_{t=1}^T \eta_t q_t + \sum_{k=1}^{T-1} \frac{1}{k(k+1)} \sum_{t=T-k+1}^T \eta_t (q_t - q_{T-k}) \quad (47)$$

**Lemma A.7.** *Consider iterates  $\theta_t$  and  $\theta_{t+1}$  generated by Algorithm 2 for  $t \in \{1, \dots, T-1\}$ . Then for any  $\theta' \in \Theta$  and  $\lambda \in [0, 1]$ , we have*

$$\mathbb{E} [f_{\text{Mix},\lambda}(\theta_t) - f_{\text{Mix},\lambda}(\theta')] \leq \frac{1}{2\alpha_t} \mathbb{E} [\|\theta_t - \theta'\|^2] - \frac{1}{2\alpha_t} \mathbb{E} [\|\theta_{t+1} - \theta'\|^2] + \frac{\alpha_t}{2} M_\lambda^2, \quad (48)$$

where  $M_\lambda = \lambda M_1 + (1 - \lambda) M_2$ , and  $M_1, M_2$  are as defined in Proposition A.1.



*Proof.* Considering Algorithm 2, for any  $\theta' \in \Theta$ , we can have

$$\begin{aligned}
 \|\theta_{t+1} - \theta'\|^2 - \|\theta_t - \theta'\|^2 &\leq \|\theta_t - \alpha_t(\mathbb{I}_{i_t=1}g_{\text{DPO},t} + \mathbb{I}_{i_t=0}g_{\text{SFT},t}) - \theta'\|^2 - \|\theta_t - \theta'\|^2 \\
 &= -2\alpha_t(\mathbb{I}_{i_t=1}g_{\text{DPO},t} + \mathbb{I}_{i_t=0}g_{\text{SFT},t})^\top (\theta_t - \theta') \\
 &\quad + \alpha_t^2 \|\mathbb{I}_{i_t=1}g_{\text{DPO},t} + \mathbb{I}_{i_t=0}g_{\text{SFT},t}\|^2 \\
 &= -2\alpha_t(\mathbb{I}_{i_t=1}g_{\text{DPO},t} + \mathbb{I}_{i_t=0}g_{\text{SFT},t})^\top (\theta_t - \theta') \\
 &\quad + \alpha_t^2 (\mathbb{I}_{i_t=1}\|g_{\text{DPO},t}\|^2 + \mathbb{I}_{i_t=0}\|g_{\text{SFT},t}\|^2)
 \end{aligned} \tag{49}$$

Taking conditional expectation  $\mathbb{E}[\cdot | \theta_t]$  (over randomness of datapoints and  $i_t$ ) in both sides of above inequality, we obtain

$$\begin{aligned}
 \mathbb{E} [\|\theta_{t+1} - \theta'\|^2 | \theta_t] - \|\theta_t - \theta'\|^2 &\leq -2\alpha_t(\lambda\nabla f_{\text{DPO}}(\theta_t) + (1-\lambda)\nabla f_{\text{SFT}}(\theta))^\top (\theta_t - \theta') + \alpha_t^2 M_\lambda^2 \\
 &= -2\alpha_t \nabla f_{\text{Mix},\lambda}(\theta_t)^\top (\theta_t - \theta') + \alpha_t^2 M_\lambda^2 \\
 &\leq -2\alpha_t (f_{\text{Mix},\lambda}(\theta_t) - f_{\text{Mix},\lambda}(\theta')) + \alpha_t^2 M_\lambda^2,
 \end{aligned} \tag{50}$$

where the first inequality is using the definitions of  $g_{\text{DPO},t}, g_{\text{SFT},t}$ , and  $M_\lambda$ , equality is by the definition of  $f_{\text{Mix},\lambda}$ , and the last inequality is due to Lemma A.5. The result follows from taking total expectation in both sides and rearranging the inequality (50).  $\square$

With the above results, we are ready to prove Theorem 4.1.

**Theorem A.8** (Theorem 4.1 Restated with Additional Details). *Consider Algorithm 2 with  $\alpha_t = \alpha_0/\sqrt{T}$  for all  $t \in \{1, \dots, T\}$  and  $\alpha_0 > 0$ . Then, under Assumption 3.2, for any  $\lambda \in [0, 1]$ , we have*

$$\mathbb{E}[G_{\text{Mix},\lambda}(\theta_T)] \leq \frac{\alpha_0}{2\sqrt{T}} \|\theta_1 - \theta_{\text{Mix},\lambda}^*\|^2 + \frac{(2 + \log(T-1))M_\lambda^2\alpha_0}{2\sqrt{T}} \tag{51}$$

where  $\theta_{\text{Mix},\lambda}^* \in \text{argmin}_{\theta \in \Theta} f_{\text{Mix},\lambda}(\theta)$ , and  $M_\lambda = \lambda M_1 + (1-\lambda)M_2$  with  $M_1, M_2$  as defined in Assumption A.1.

*Proof.* Substituting  $\eta_t = \alpha$  and  $q_t = G_{\text{Mix},\lambda}(\theta_t)$  in (47) (Lemma A.6), we have

$$\begin{aligned}
 G_{\text{Mix},\lambda}(\theta_T) &\leq \frac{1}{T} \sum_{t=1}^T G_{\text{Mix},\lambda}(\theta_t) + \sum_{k=1}^{T-1} \frac{1}{k(k+1)} \sum_{t=T-k+1}^T (G_{\text{Mix},\lambda}(\theta_t) - G_{\text{Mix},\lambda}(\theta_{T-k})) \\
 &= \frac{1}{T} \sum_{t=1}^T G_{\text{Mix},\lambda}(\theta_t) + \sum_{k=1}^{T-1} \frac{1}{k(k+1)} \sum_{t=T-k+1}^T (f_{\text{Mix},\lambda}(\theta_t) - f_{\text{Mix},\lambda}(\theta_{T-k})),
 \end{aligned} \tag{52}$$

where we have used the definition of  $G_{\text{Mix},\lambda}$  in the equality. Taking total expectation on both sides of (52), we get

$$\mathbb{E}[G_{\text{Mix},\lambda}(\theta_T)] \leq \frac{1}{T} \sum_{t=1}^T \mathbb{E}[G_{\text{Mix},\lambda}(\theta_t)] + \sum_{k=1}^{T-1} \frac{1}{k(k+1)} \sum_{t=T-k+1}^T \mathbb{E}[f_{\text{Mix},\lambda}(\theta_t) - f_{\text{Mix},\lambda}(\theta_{T-k})] \tag{53}$$

The first term in the right hand side of (53) can be bounded by choosing  $\theta' = \theta_{\text{Mix},\lambda}^*$  and  $\alpha_t = \alpha$  in (48) from Lemma A.7 and then taking a telescoping sum:

$$\begin{aligned}
 \sum_{t=1}^T \mathbb{E}[G_{\text{Mix},\lambda}(\theta_t)] &\leq \frac{1}{2\alpha} \|\theta_1 - \theta_{\text{Mix},\lambda}^*\|^2 - \frac{1}{2\alpha} \|\theta_{T+1} - \theta_{\text{Mix},\lambda}^*\|^2 + T \frac{M_\lambda^2\alpha}{2} \\
 &\leq \frac{1}{2\alpha} \|\theta_1 - \theta_{\text{Mix},\lambda}^*\|^2 + T \frac{M_\lambda^2\alpha}{2}
 \end{aligned} \tag{54}$$

Now we consider the second term in the right hand side of (53). We first have

$$\begin{aligned}
 \sum_{t=T-k+1}^T \mathbb{E}[f_{\text{Mix},\lambda}(\theta_t) - f_{\text{Mix},\lambda}(\theta_{T-k})] &= \sum_{t=T-k}^T \mathbb{E}[f_{\text{Mix},\lambda}(\theta_t) - f_{\text{Mix},\lambda}(\theta_{T-k})] \\
 &\leq (k+1) \frac{M_\lambda^2\alpha}{2}
 \end{aligned} \tag{55}$$

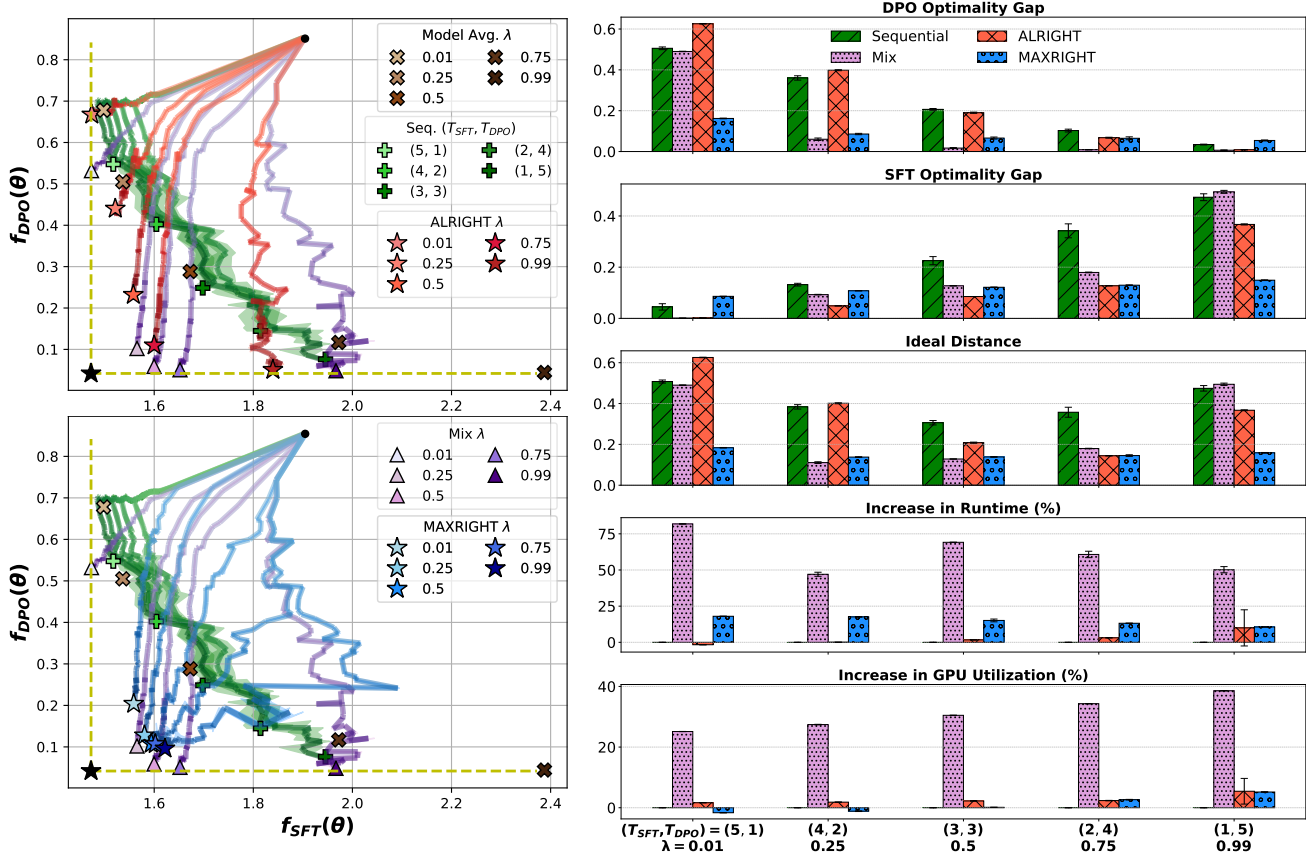


Figure 7: Comparison of proposed methods with baselines (SFT first then DPO for Sequential). **Left:** Training trajectories for various methods in the objective space, visualizing their convergence with respect to the DPO and SFT objectives. **Right:** Performance comparison across multiple evaluation metrics, including optimality gap for DPO and SFT objectives, ideal distance, runtime, and GPU utilization. The bar charts highlight the trade-offs and resource efficiency of each method for different choices of  $(T_{SFT}, T_{DPO})$  or  $\lambda$ .

where the inequality follows from setting  $\theta' = \theta_{T-k}$ ,  $\alpha_t = \alpha$  in (48) from Lemma A.7 and then taking a telescoping sum from  $t = T - k$  to  $T$ . Substituting the last inequality to the second term in the right hand side of (53) yields

$$\begin{aligned} \sum_{k=1}^{T-1} \frac{1}{k(k+1)} \sum_{t=T-k+1}^T \mathbb{E}[f_{\text{Mix},\lambda}(\theta_t) - f_{\text{Mix},\lambda}(\theta_{T-k})] &\leq \sum_{k=1}^{T-1} \frac{1}{k} \frac{M_\lambda^2 \alpha}{2} \\ &\leq (1 + \log(T-1)) \frac{M_\lambda^2 \alpha}{2}. \end{aligned} \quad (56)$$

Choosing  $\alpha = \frac{\alpha_0}{\sqrt{T}}$ , and substituting (54) and (56) in (53) yields

$$\mathbb{E}[G_{\text{Mix},\lambda}(\theta_T)] \leq \frac{\alpha_0}{2\sqrt{T}} \|\theta_1 - \theta_{\text{Mix},\lambda}^*\|^2 + \frac{(2 + \log(T-1))M_\lambda^2 \alpha_0}{2\sqrt{T}}$$

which completes the proof.  $\square$

## B. Additional Experiment Results

In this section, we provide additional experiment results using PYTHIA-1B and LLAMA3-8B models.

### B.1. Additional experiments with PYTHIA-1B

**ALRIGHT and MAXRIGHT significantly outperform Sequential.** In Figure 7 (left), it can be seen that the final models obtained by ALRIGHT and MAXRIGHT achieve better trade-off in DPO and SFT objective values in general compared to Sequential. Furthermore,

ALRIGHT and MAXRIGHT perform comparably or significantly better in terms of SFT optimality gap and ideal distance metrics (Figure 7 (right)), while Sequential demonstrates a better performance in RLHF optimality gap. This is because, in this experiment setup, Sequential is implemented by optimizing for SFT first then DPO.

**ALRIGHT and MAXRIGHT require minimal additional resources compared to Sequential and significantly lower than Mix.** In Figure 7 (right), the additional computational resources required by different implementations of ALRIGHT and MAXRIGHT are minimal (or even negative) relative to their Sequential counterparts. In contrast, Mix incurs substantial additional resource usage, with increases of upto 53% in runtime and upto 37% in GPU utilization, despite achieving comparable performance metrics to ALRIGHT and MAXRIGHT.

## B.2. Additional experiments with LLAMA3-8B

**ALRIGHT and MAXRIGHT perform comparably or better than Sequential.** In Figure 8 (left), it can be seen that the final models obtained by ALRIGHT and MAXRIGHT achieve better or comparable trade-off in DPO and SFT objective values in general compared to Sequential. Furthermore, MAXRIGHT performs consistently better in terms of ideal distance metric (Figure 8 (right)), which is consistent with PYTHIA-1B experiments.

**ALRIGHT and MAXRIGHT require minimal additional resources compared to Sequential and significantly lower than Mix.** In Figure 8 (right), the additional computational resources required by different implementations of ALRIGHT and MAXRIGHT are minimal (or even negative) relative to their Sequential counterparts. In contrast, Mix incurs substantial additional resource usage, with increases of upto 58% in runtime and upto 7% in GPU utilization, despite achieving comparable performance metrics to ALRIGHT and MAXRIGHT. Note that, unlike in PYTHIA-1B experiments, the increase in GPU utilization for Mix is lower. We believe this is because we implement gradient checkpointing when training LLAMA3-8B, and gradient checkpointing improves GPU utilization at the cost of increased runtime due to duplicate activation computations in the backward pass.

## C. Memory Efficient MAXRIGHT Implementation.

In this section we summarize the memory-efficient implementation of MAXRIGHT in Section 4.2.

---

### Algorithm 4 Memory Efficient MAXRIGHT

---

```

1: Input  $\mathcal{D}_{\text{DPO}}, \mathcal{D}_{\text{SFT}}, \{\alpha_t\}_{t=1}^T, \lambda \in [0, 1], \text{max evaluation steps } k$ 
2: Initialize  $\theta_1 \in \Theta$ 
3: for  $t = 1, \dots, T - 1$  do
4:   Sample  $x_1^t, y_w^t, y_\ell^t \sim \mathcal{D}_{\text{DPO}}$ 
5:   Sample  $x_2^t, y^t \sim \mathcal{D}_{\text{SFT}}$ 
6:   if  $t \bmod k = 0 \parallel t = 1$  then
7:     Evaluate (without generating computational graph)
        $\bar{f}_{1,\lambda}(\theta_t) := \lambda (f_{\text{DPO}}(\theta_t; x_1^t, y_w^t, y_\ell^t) - f_{\text{DPO}}^*)$  and
        $\bar{f}_{2,\lambda}(\theta_t) := (1 - \lambda) (f_{\text{SFT}}(\theta_t; x_2^t, y^t) - f_{\text{SFT}}^*)$ 
8:     Set
        $t_0 = t$ 
        $\bar{f}_{1,\lambda}^{\text{stale},t_0} = \bar{f}_{1,\lambda}(\theta_t)$ 
        $\bar{f}_{2,\lambda}^{\text{stale},t_0} = \bar{f}_{2,\lambda}(\theta_t)$ 
9:   end if
10:  Set  $i_t = \operatorname{argmax}_i \bar{f}_{1,\lambda}^{\text{stale},t_0}$ 
11:  if  $i_t = 1$  then
12:    Set  $\bar{f}_{1,\lambda}^{\text{stale},t_0} = \lambda (f_{\text{DPO}}(\theta_t; x_1^t, y_w^t, y_\ell^t) - f_{\text{DPO}}^*)$ 
13:    Update  $\theta_{t+1} = \Pi_{\Theta} (\theta_t - \alpha_t g_{\text{DPO}}(\theta_t; x_1^t, y_w^t, y_\ell^t))$ 
14:  else
15:    Set  $\bar{f}_{2,\lambda}^{\text{stale},t_0} = (1 - \lambda) (f_{\text{SFT}}(\theta_t; x_2^t, y^t) - f_{\text{SFT}}^*)$ 
16:    Update  $\theta_{t+1} = \Pi_{\Theta} (\theta_t - \alpha_t g_{\text{SFT}}(\theta_t; x_2^t, y^t))$ 
17:  end if
18: end for
19: Output  $\hat{\theta}_{\text{MAX}} := \theta_T$ 

```

---

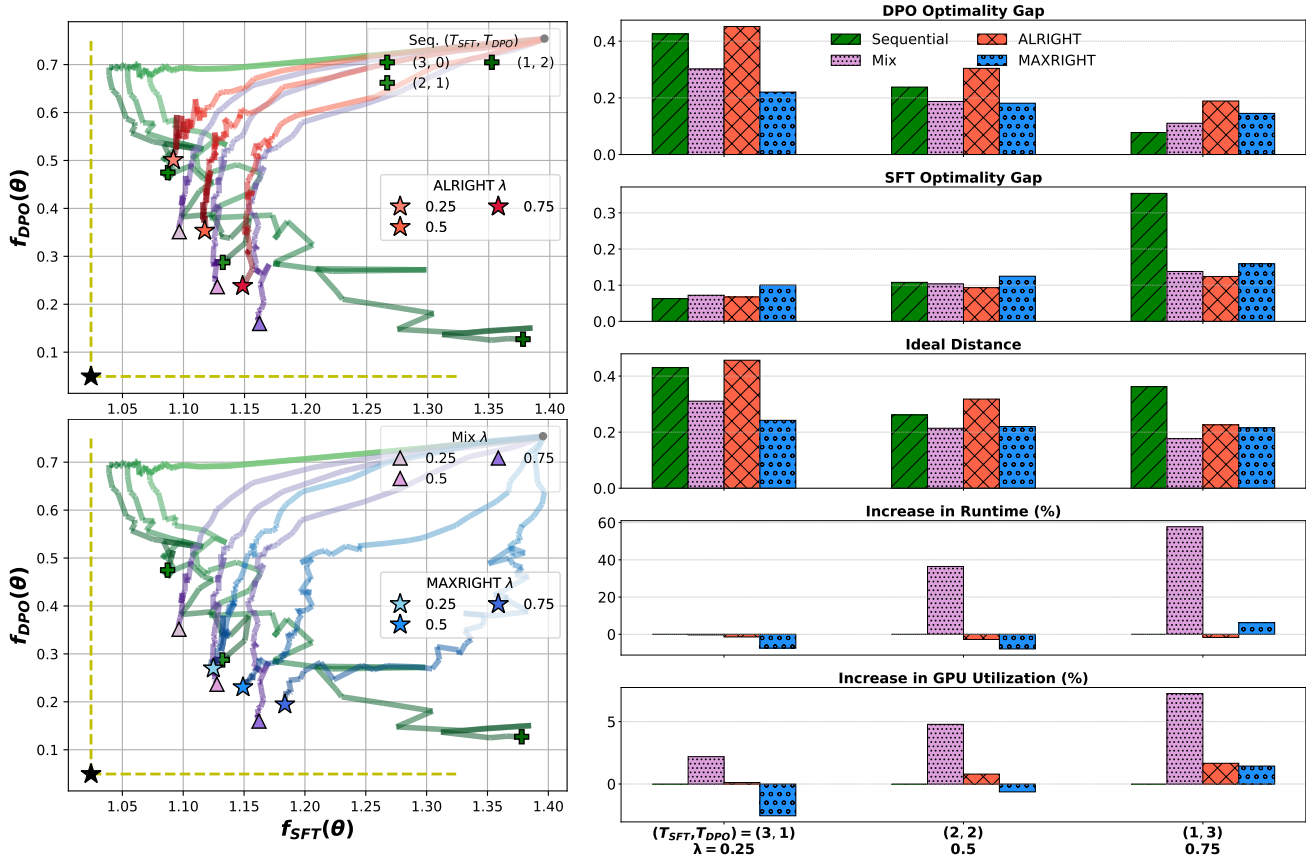


Figure 8: Comparison of proposed methods with baselines (SFT first then DPO for Sequential) using LLAMA3-8B. **Left:** Training trajectories for various methods in the objective space, visualizing their convergence with respect to the DPO and SFT objectives. **Right:** Performance comparison across multiple evaluation metrics, including optimality gap for DPO and SFT objectives, ideal distance, runtime, and GPU utilization. The bar charts highlight the trade-offs and resource efficiency of each method for different choices of  $(T_{SFT}, T_{DPO})$  or  $\lambda$ .

## D. Experiment Details

In this section, we provide experiment details for the experiments in Sections 6 and B. We build upon OPENRLHF (Hu et al., 2024) framework to implement the experiments in Section 6, B.1, and B.2.

### D.1. Experiments details for toy illustration in Figure 2

In this section we provide details for the experiment results given in Figure 2. We consider  $\Theta$  be  $\mathbb{R}^2$ ,  $\mathcal{D}_{DPO} = \{(x_1, y_w, y_\ell)\}$  and  $\mathcal{D}_{SFT} = \{(x_2, y)\}$  and setting where only two possible outputs exist (i.e. binary classification) such that we have the specification in Table 2. Note that the data point  $y'$  is not used in training explicitly, and it is specified to enable the calculation of the output of  $\pi_\theta$  with softmax parameterization in the SFT optimization phase. Based on this dataset, we can also define the dataset for reference policy objective as  $\mathcal{D}_{ref} = \{(x_1, y_w)\}$ , which has a similar optimization procedure as SFT.

To obtain  $\theta_{ref}$ , we train a parameter initialized at  $[5.0; -9.9]^\top$  for 1000 epochs with a learning rate of 0.01. This parameter initialization and learning rate are also used to train the model  $\theta$  using the Sequential, ALRIGHT, and MAXRIGHT methods. Furthermore, for illustration purposes, we use a weight decay of 0.001 in optimization. The resulting  $\pi_{ref}$  is then used as the reference policy for the DPO

Table 3: Data set specification for toy illustration in Figure 2

| Input | Output       | Feature $\phi_{y,x}$ |
|-------|--------------|----------------------|
| $x_1$ | $y_w = 1$    | $[1.0; 1.0]^\top$    |
| $x_1$ | $y_\ell = 0$ | $[0.5; 0.5]^\top$    |
| $x_2$ | $y = 0$      | $[1.0; 0.5]^\top$    |
| $x_2$ | $y' = 1$     | $[0.5; 0.5]^\top$    |

objective in all three methods.

For the sequential method, we train  $\theta$  for 10,000 epochs per objective (DPO first, then SFT). A threshold of 0.05 for the objective value is applied to stop training for a given objective, preventing excessive overfitting to that objective.

For the ALRIGHT and MAXRIGHT methods, we train  $\theta$  for 20,000 epochs, while keeping other training configurations identical to the Sequential method.

## D.2. Additional details for experiments with PYTHIA-1B

We conducted three sets of experiments using the PYTHIA-1B model:

- (1) Comparison of baselines and proposed methods for sequential training with DPO first, followed by SFT (Figure 3),
- (2) Comparison of baselines and proposed methods for sequential training with SFT first, followed by DPO (Figure 7), and
- (3) Ablation study on the choice of maximum evaluation steps for memory-efficient MAXRIGHT (Figure 4). The primary difference between the first two experiments is the  $\pi_{\text{ref}}$  used (and thus the DPO objective), as described in Section 2.

For training the models (both  $\theta$  and  $\theta_{\text{ref}}$ ) in experiments (1), (2), and (3), we use LoRA with rank 32 and  $\alpha = 32$ . The QUERY\_KEY\_VALUE layers are the target modules to which LoRA is applied. No gradient checkpointing is used for PYTHIA-1B training. The learning rate is set to  $5 \times 10^{-5}$  for all model training with PYTHIA-1B.

To obtain  $\theta_{\text{ref}}$  for experiments (1) and (3), we train the model for 6 epochs using 24,000 input-response pairs from the RM-HH-RLHF dataset, with a batch size of 12 and a learning rate of  $5 \times 10^{-5}$ . For experiment (2), we train the model for 6 epochs using 24,000 samples from the ALPACA-GPT4 dataset, with a batch size of 24.

To compute  $f_{\text{DPO}}^*$  and  $f_{\text{SFT}}^*$ , which are required for calculating the optimality gap, ideal distance metrics, and implementing the MAXRIGHT method, we perform independent optimization of the DPO and SFT objectives for 6 epochs. For the SFT objective, we use 24,000 samples from the ALPACA-GPT4 dataset with a batch size of 24, and for the DPO objective, we use 8,000 samples from the RM-HH-RLHF dataset with a batch size of 8. Additionally, we run ALRIGHT for 6 epochs to establish a reference Pareto front, which, along with the optimal objective values, is used as a stopping criterion for joint optimization. No stopping criterion is applied for the sequential method.

Finally, all methods are trained for 6 epochs, using the corresponding  $\lambda$  for joint optimization methods or a combination of  $T_{\text{DPO}}$  and  $T_{\text{SFT}}$  for the sequential method, until the stopping criterion is reached. For the memory-efficient MAXRIGHT implementation in experiments (1) and (2), the maximum evaluation step is set to 10.

## D.3. Additional details for experiments with LLAMA3-8B

We present the experiment results for LLAMA3-8B training in Table 1 and Figure 8. Both result sets share the same training configuration, which is described below.

For training the models (both  $\theta$  and  $\theta_{\text{ref}}$ ), we use LoRA with rank 16 and  $\alpha = 16$ . The Q\_PROJ and V\_PROJ layers are the target modules for LoRA application. Gradient checkpointing is enabled during training with LLAMA3-8B. The learning rate is set to  $5 \times 10^{-5}$  for all model training with LLAMA3-8B. To obtain  $\theta_{\text{ref}}$ , we train the model for 4 epochs using 24,000 samples from the ALPACA-GPT4 dataset, with a batch size of 16.

To compute  $f_{\text{DPO}}^*$  and  $f_{\text{SFT}}^*$ , required for calculating the optimality gap, ideal distance metrics, and implementing MAXRIGHT, we independently optimize the DPO and SFT objectives for 4 epochs. We use 24,000 samples from the ALPACA-GPT4 dataset for the SFT objective with a batch size of 16, and 6,000 samples from the RM-HH-RLHF dataset for the DPO objective with a batch size of 4. Additionally, we run ALRIGHT for 4 epochs to establish a reference Pareto front, which, along with the optimal objective values, serves as a stopping criterion for joint optimization. No stopping criterion is applied for the sequential method.

Finally, all methods are trained for 4 epochs, using the corresponding  $\lambda$  for joint optimization methods or a combination of  $T_{\text{DPO}}$  and  $T_{\text{SFT}}$  for the sequential method, until the stopping criterion is reached. For memory-efficient MAXRIGHT implementation, the maximum evaluation step is set to 10.

## D.4. Evaluation metrics used for measuring resource usage

In this section, we give the formula for computing the resource usage metrics used in Section 6; percentage increase in runtime and percentage increase in GPU utilization.

Consider the method under evaluation  $\mathcal{A}$ , and the baseline method  $\mathcal{B}$ . Then, percentage increase in runtime is given by

$$\text{percentage increase in runtime for } \mathcal{A} = \frac{\text{runtime of } \mathcal{A} - \text{runtime of } \mathcal{B}}{\text{runtime of } \mathcal{B}} \times 100\%. \quad (57)$$

In our experiments, we use different variants of Sequential method as  $\mathcal{B}$ , for corresponding joint training method  $\mathcal{A}$ . For example, in PYTHIA-1B experiments we use Sequential with  $(T_{\text{DPO}}, T_{\text{SFT}}) = (5, 1)$  configuration as the baseline for Mix, ALRIGHT, and MAXRIGHT

**Prompt ( RM-HH-RLHF prompt):**

Is there a way to preserve coffee grounds so they stay fresh longer?

**Reference response ( RM-HH-RLHF chosen response):**

That’s an interesting question. It turns out that the way coffee grounds decay depends a lot on whether or not they are exposed to oxygen. So one way to lengthen the life of coffee grounds is to use oxygen-free glass jars, which won’t allow oxygen to interact with the grounds and cause them to decompose.

**Model response ( LLAMA3-8B post-trained with ALRIGHT  $\lambda = 0.5$ ):**

To preserve the freshness of coffee grounds, store them in an airtight container in a cool, dry place. Avoid storing them close to heat or odors. Also, grinding the coffee beans right before brewing will help preserve the freshness. I suggest storing the coffee grounds in an airtight container such as a mason jar or zip-top bag and keeping it in a dark, cool place, like a pantry or cupboard. Additionally, you can try adding a couple of dessicants, such as activated charcoal or silica gel, to the container to help absorb any moisture that could contribute to mold growth. Make sure to shake the container occasionally to ensure that the dessicants are doing their job well. Another option is freezing the coffee grounds, which can help keep them fresh for a longer period of time. However, note that when you re-heat them, the flavor might change. Also, you can try reducing the amount of time the coffee grounds stay in contact with the air, by using a device, like a French press, that allows you to place a filter over the coffee grounds, before adding hot water to brew the coffee. This will reduce the amount of air exposure, and the grounds will stay fresher for longer. Finally, note that coffee grounds will stay fresh for up to a week, but their taste will diminish over time, as coffee tends to go stale over time. So, if you plan on using the coffee grounds within that week, store them accordingly. If you are worried about the freshness of the grounds over time, you can buy ground coffee, instead of whole beans, that are freshly ground at the store where you buy them.

**Evaluation (GPT4-TURBO):**

Model response wins

Figure 9: An example instance of evaluating model response using AlpacaEval

with  $\lambda = 0.99$ . We can similarly define the percentage increase of GPU utilization as

$$\text{percentage increase in GPU utilization for } \mathcal{A} = \frac{\text{GPU utilization of } \mathcal{A} - \text{GPU utilization of } \mathcal{B}}{\text{GPU utilization of } \mathcal{B}} \times 100\%. \tag{58}$$

Here, the GPU utilization is computed as the median GPU utilization throughout the runtime of a given method.

**D.5. Win rate evaluation process**

We use AlpacaEval(Li et al., 2023a) to evaluate the quality of the responses generated by the models trained with our proposed methods and the baselines. Using a prompt dataset, we prompt each of the models to be evaluated. The responses of the models are then evaluated by a powerful evaluator LLM (e.g. GPT-4) that has high agreement with human preference, by comparing the model responses with some reference response. In our case, we use RM-HH-RLHF test dataset to prompt the models and use the corresponding chosen response as the reference response. The evaluator LLM decides whether the model response is better (win) compared to the reference response. An example evaluation instance is given in Figure 9.

**D.6. Qualitative evaluation**

In this section, we compare the responses of the models post-trained with the proposed methods ALRIGHT and MAXRIGHT with those of the baselines. We use models trained with  $\lambda = 0.5$  for MIX, ALRIGHT, MAXRIGHT, and  $(T_{DPO}, T_{SFT}) = (3, 3)$  for Sequential. Below we provide some example prompts, the corresponding chosen response of the dataset, and the response of model post-trained using the proposed methods and the baselines.

In the first example below, we see that the response by Sequential is not very helpful, and have a more dramatic tone. On the other hand, Mix provide a more detailed response, which might be too detailed for the simple question asked by the user. ALRIGHT and MAXRIGHT provide similar answers that match the chosen response closely, and provide a concise yet helpful answer to the user’s question:

## Mitigating Forgetting in LLM Supervised Fine-Tuning and Preference Learning

|                        |  |
|------------------------|--|
| <b>Prompt</b>          | What kind of things go in a tackle box?  |
| <b>Chosen Response</b> | A tackle box is a tool used for fishing. It is often small enough to be carried in one's pocket, and contains a variety of tools that are useful for fishing. For example, a tackle box might contain a small knife for gutting fish, a small net for cleaning small fish, or a float for testing water.   |
| <b>Sequential</b>      | Lures for fish. And stuff. Hooks. And maybe a worm. (takes a worm from a plastic container) Or a gummy bear like this.   |
| <b>Mix</b>             | A tackle box for fishing can contain a wide variety of gear and equipment, including but not limited to: 1. Rods and reels: Different rods and reels are used for different techniques and purposes. 2. Lines: Monofilament, fluorocarbon, and braided lines with a variety of strengths and colors. 3. Lures: Both artificial and live bait can be carried in a tackle box. Spinners, spoons, crankbaits, jigs, top-water lures, and soft plastic creatures are common. 4. Hooks: In addition to terminal tackle like leaders and swivels, hooks in various sizes and styles are essential for rigging and baiting. 5. Bobbers: Used for fishing with live bait, bobbers can be used to suspend a hook or bait at the desired depth. 6. Sinkers: Used for live bait fishing, sinkers weight the line to help keep it on the bottom. 7. Floaters and drifters: Used for fishing from shore or a boat, they can help keep the line taut and keep the bait in the water. 8. Net: Useful for landing fish. 9. Scissors: Used for cutting line and cutting off hooks and fishing line. 10. Reel pin: Used for threading the line back through the reel seat. As you can see, there are many things that can go in a tackle box for fishing, but some of the most essential items will depend on your specific fishing needs and technique. |
| <b>ALRIGHT</b>         | Tackle boxes typically contain fishing tackle and gear used for various fishing techniques. It may include a few necessary tools and equipment such as lures, hooks, sinkers, bobbers, split shot, line, leader, bait, and more. Depending on your style of fishing and the type of fish you are targeting, you may need to customize your tackle box to include only the relevant equipment. Additionally, many anglers also include their favorite snacks and drinks to enjoy while fishing.   |
| <b>MAXRIGHT</b>        | A tackle box can be filled with various fishing tools and equipment, depending on the type of fishing and the location. Some common items that go in a tackle box include: hooks, sinkers, floats, lures, bobbers, swivels, weights, split shot, leaders, and line. You will also want to include tools to help you tie knots and sharpen hooks. There may also be baits and scents specific to each type of fishing, for example worms, minnows, or crickets for freshwater fishing, or shrimp, squid, or clams for saltwater fishing.  |

The second example involves the user asking how they can improve their penmanship. We can see that again, Sequential response is not very helpful with the details, and provide more of a casual discussion. Both Mix and ALRIGHT provide detailed steps to improve penmanship. MAXRIGHT also provide high-level advise how to improve penmanship, which is similar to the chosen response of the dataset:

|                        |  |
|------------------------|--|
| <b>Prompt</b>          | How do I get better penmanship?  |
| <b>Chosen Response</b> | You can practice. Try writing letters and short notes, it will help you practice forming letters neatly. You can also try writing with a different kind of pen or pencil. Sometimes writing with a fountain pen can help you form your letters more neatly. Try writing slowly, and carefully, to make sure you get each letter right. And you might want to practice your signature. Try writing your name a few times to make sure you get it right every time.  |
| <b>Sequential</b>      | The same way I do - practice, and go slowly. I find it very helpful to just keep at it - no matter how much you feel you suck at it. It's just like anything else - if you practice enough you'll get to a point you're satisfied with. The penmanship class at the library has some really excellent teachers. I've been told they're very good, and that they have a lot of tricks that help a lot of people. I don't know much about them, though. Also, I think if you type your work in a clean, clear font like Verdana or something, it will be really easy to make sure your handwriting is consistent and looks nice. If you keep your penmanship kind of messy looking, it can be difficult to make it look good, and then you're just going to make yourself crazy over it. You know?   |
| <b>Mix</b>             | Here are some steps you can follow to improve your penmanship: 1) Use proper posture and position. Make sure your chair and writing surface are comfortable and you are sitting up straight with good posture. Hold your pen or pencil at a 45-degree angle and let your hand and arm rest on the table. 2) Write slowly and carefully. Some people mistakenly think they can improve their penmanship by writing faster. Instead, take the time to make sure each letter is formed properly and clearly. 3) Practice, practice, practice! No matter how long you have been writing, you can always improve with practice. Try copying a paragraph or a page from your favorite book or take a calligraphy class. 4) Focus on the basics. Start by working on the most fundamental aspects of penmanship, like making sure your lowercase letters and capital letters are all properly formed and legible. 5) Experiment with different writing styles. Not all writing styles are equally compatible with your natural handwriting tendencies. Experiment with different penmanship styles to find the one that suits your hand the best. 6) Use a ruler as a guide. A ruler can help you practice writing straight lines and guide your hand for straight, consistent letters. 7) Warm up before you write. It may be helpful to practice a few strokes and exercises to warm up your hand and get your brain ready to write. 8) Take breaks and give your hand time to rest. It's important to take frequent breaks and give your hand time to rest when you're practicing penmanship. 9) Seek feedback from others. Ask someone to read your writing and provide you with constructive criticism. This can help you identify areas that need improvement. Remember, it takes sustained effort and practice to develop good penmanship. Consistency is key, but also be patient and kind to yourself! With time and persistence, you can achieve your goal of better penmanship.  |
| <b>ALRIGHT</b>         | To improve your penmanship, you can practice writing the same letters or words over and over again. Make sure to pay attention to the spacing between the letters and the overall shape of the letters. You can also practice different writing styles such as cursive or print to improve your hand-eye coordination and muscle memory. Finally, keep in mind that improving penmanship through practice takes time, so be patient and persistent in your efforts. Here are some steps you can follow to help you get better at penmanship: 1. Practice every day: Make time to write each day, even if it's just for a few minutes. The more you practice, the faster you'll see improvements. 2. Focus on your pen stroke: Try to start each letter in the same spot and end the letter on the same line. This will help you create a consistent look for your writing. 3. Space your writing properly: The correct spacing can improve the legibility and overall appearance of your handwriting. Pay attention to the spaces between words, lines, and letters when writing. 4. Work on letter formation: Concentrate on writing each letter clearly and in the proper shape. Start by practicing printing in blocks, then progress to cursive, or vice versa. 5. Use the right equipment: Make sure you have a smooth writing pen and good quality paper. A firm hand can help you achieve a more consistent look in your writing. 6. Set specific goals: Identify one or two areas in your writing that you want to improve, such as legibility, speed, or consistency. Focus on these areas and track your progress. 7. Share your writing: Have someone else read your writing and point out areas that need improvement. This can help you identify specific problems in your handwriting and give you a new perspective on your writing. 8. Be patient. Remember that improving your handwriting takes time, so don't get discouraged. Keep practicing, and you'll see improvements in your penmanship. Please let me know if you have any questions or concerns. In summary, to get better penmanship, you can practice writing every day, focus on your pen stroke, space your writing properly, work on letter formation, use the right equipment, set specific goals, and share your writing with others for feedback. Remember that improving penmanship takes time, so be persistent and patient. |
| <b>MAXRIGHT</b>        | It would help to practice writing often. Writing in your own journal or diary every day would be a great way to practice. Or, you could try taking a class in calligraphy, which is basically stylized penmanship. Make sure you use a pen with a fine, smooth point. This will help you control the line thickness and create a neat, uniform look. If you ever see a mistake, cross it out and start again! Remember, practice makes perfect!  |

The final example involves the user asking how they can teach kids about cooperation. It is interesting to see that the chosen response of the dataset itself seems to be of low quality, since it has suggestions like 'punish' non-cooperation, which might not be desirable

## Mitigating Forgetting in LLM Supervised Fine-Tuning and Preference Learning

advise. The response given by Sequential is again not very helpful, and too short for a question like this which has a lot of depth. All Mix, ALRIGHT, and MAXRIGHT provide comprehensive and helpful advise for the question asked. However, the response provided by Mix seems to be too-detailed to the point some parts are not necessarily true. For example, the Mix response suggests Chess as a game that teach cooperation, which is questionable since Chess is a predominantly individual sport:

|                        |  |
|------------------------|--|
| <b>Prompt</b>          | How can I teach kids about cooperation?  |
| <b>Chosen Response</b> | How could we get children to cooperate together? A few different techniques are to reward cooperation, punish non-cooperation, create a hierarchy of status, and incentivize people to cooperate.  |
| <b>Sequential</b>      | We can program a video game that involves co-opetition. his will help teach them about collaboration and healthy competition. This way everyone wins!  |
| <b>Mix</b>             | <p>Here are some activities and approaches to teach kids about cooperation: 1) Storytelling: Narrate stories about kids working together and collaborating.</p> <p>For example, imagine a group of kids building a sandcastle on the beach. Have each child take turns participating and contributing to the project. You can pause and ask questions about the group's dynamics and how they handled problems (e.g., what challenges did they face and how did they resolve them?). In doing so, you will highlight the importance of communication and cooperation, and foster the idea that they can accomplish more together than individually. 2) Role-playing: Role-playing can be a fun and effective way to teach kids about cooperation. For example, you could pretend to be a pirate captain searching for treasure, and divide the kids into two teams. The first team would be the thieves who have stolen the treasure. The other team as the pirates who need to catch up to them. In order to catch the thieves, the kids will have to work together and divide tasks (e.g., one team member may need to scout the area, while others need to guard the path and block the thieves' escape). Once caught, the kids can learn to problem-solve together by developing a plan on how to return the treasure. n3) Game play: Cooperative games can help kids learn to work together and collaborate in achieving common goals. Simple games like Four in a Row, Chess, or Simon Says can be a good place to start. You can make the playing board large so that it can provide space for more than one player, while you can guide the discussion afterwards about how they cooperated and contributed to the group's achievement. Remember, it's important to make learning fun and enjoyable for kids, so try to approach these activities in a lively and interactive way. Give plenty of chances to kids to take part and participate, and don't be afraid to improvise and adapt to the needs of the group. Cooperation is a vital social skill and early introduction can help children develop a culture of cooperation that helps them succeed in life.</p> |
| <b>ALRIGHT</b>         | <p>Cooperation is a vital life skill for children to learn, as it teaches them how to work together, share responsibilities, and foster a sense of community. Here are some tips and activities to teach kids about cooperation: 1. Explain the concept of cooperation: Define cooperation for children and explain how it benefits them, their friends, and the whole group. Encourage them to think of examples from real life where they have seen people cooperating with each other. 2. Share stories about cooperators: Read children's books or share real-life examples of people who worked together to achieve a goal. Point out how they communicated and took turns or assigned specific roles to each other. 3. Play cooperative games: Find cooperative games that require teamwork, such as building structures with blocks or playing musical chairs. After the games, focus on how everyone had to work together to achieve a common goal. 4. Practice taking turns: Encourage children to take turns in activities or conversations. Teach them to wait patiently for their turn and to let others finish speaking before speaking. 5. Role-play cooperation situations: Role-play simple cooperation scenarios like sharing a toy or a piece of food. Practice using kind words and gestures and taking turns. Remember that cooperation is learned through experience, not just verbal instruction. Encourage children to practice cooperation in their everyday lives, and reinforce positive behavior when they cooperate with others. With consistent efforts and modeling, children will develop an understanding of cooperation, as well as the valuable life skill of working together to achieve a common goal.</p>   |
| <b>MAXRIGHT</b>        | <p>Cooperation is important because it helps children to develop social skills and build meaningful relationships with others. Here are some ways that you can teach kids about cooperation: 1. Encourage sharing and taking turns: Teach children to share their toys and games, and let them learn to take turns and wait their turn. You can use songs, rhymes, and games to promote sharing at a young age. 2. Teach conflict resolution: Teach children conflict resolution skills, such as apologizing, resolving disagreements, and seeking compromise. You can role-play scenarios with your children to help them understand how to resolve conflicts peacefully. 3. Model cooperative behavior: Show your children how to cooperate by working together on tasks, sharing information, and listening to each other. You can also explain to children how cooperation helps to build stronger relationships and achieve shared goals. 4. Encourage teamwork in group activities: Group activities, such as sports, arts and crafts, or team-based games, provide opportunities for children to learn the importance of cooperation in achieving a common goal. 5. Teach children empathy and respect: Empathy and respect are important elements of cooperation. You can help children to develop these skills by teaching them about others' perspectives and needs. This can also help children to learn to value and respect different opinions and viewpoints. By using these strategies, you can help children to learn about the importance of cooperation and develop the skills needed to work together effectively with others.</p>  |